PREHNITE DISSOCIATION CURVE BELOW 3 KILOBARS WATER PRESSURE

by

Wayne Edward Colony

A Thesis Submitted to the Faculty of the

DEPARTMENT OF GEOLOGY

In Partial Fulfillment of the Requirements
For the Degree of

MASTER OF SCIENCE

In the Graduate College

THE UNIVERSITY OF ARIZONA

1970

STATEMENT BY AUTHOR

This thesis has been submitted in partial fulfillment of requirements for an advanced degree at The University of Arizona and is deposited in the University Library to be made available to borrowers under rules of the Library.

Brief quotations from this thesis are allowable without special permission, provided that accurate acknowledgment of source is made. Requests for permission for extended quotation from or reproduction of this manuscript in whole or in part may be granted by the head of the major department or the Dean of the Graduate College when in his judgment the proposed use of the material is in the interests of scholarship. In all other instances, however, permission must be obtained from the author.

SIGNED: Wayne Colby

APPROVAL BY THESIS DIRECTOR

This thesis has been approved on the date shown below:

BERT E. NORDLIE
Assistant Professor of Geology

May 6, 1970
Date

ACKNOWLEDGMENTS

Special gratitude is given to Dr. Bert E. Nordlie, whose unceasing enthusiasm and effort made this investigation possible and opened many new doors to the future. Appreciation is also expressed for the encouragement and interest shown during this investigation by Dr. Richard F. Wilson and Dr. John W. Anthony.

The author also wishes to thank The Society of Sigma Xi for their helpful financial assistance. I am particularly grateful to my wife, Charlotte, who gave many hours of helpful assistance in completing this thesis.

TABLE OF CONTENTS

TABLE OF CONTENTS--Continued

LIST OF ILLUSTRATIONS

LIST OF ILLUSTRATIONS--Continued

LIST OF TABLES

ABSTRACT

Prehnite dissociates to form wollastonite, anorthite, and grossularite. The formation of the grossularite is considered as the result of the prehnite not being stoichiometric. Dissociation of prehnite occurs at 475°C and 1000 bars water pressure. Kinetics prohibit obtaining experimental data below 800 bars water pressure, however the dissociation curve is extrapolated to low water pressures. This extrapolation is based on quantitative thermodynamic calculations. At low water pressures the curve becomes tangential to the H_2O-liquid H_2O-vapor phase boundary.

Prehnite can form from CaO-SiO_2 metasomatism of Ca-rich plagioclase in nearly all rock types, including basalts, andesites, diorites, gabbros, diabases, graywackes, and volcanic sediments. Based on geologic evidence, prehnite in basalt amygdales must have formed at 1 atmosphere water pressure and less than 100°C. The compositional dependence of the dissociation curve suggests that prehnite may not be a good index mineral to use in defining low-grade metamorphic facies. Further experimental work is required using mineral assemblages before prehnite can be used meaningfully as an index mineral.

CHAPTER 1

INTRODUCTION

The widespread occurrence of prehnite in low-grade metamorphic environments has been known for many years. However, it was not until Coombs (1960) proposed the prehnite-pumpellyite metagraywacke facies that general petrological interest in prehnite was aroused. Coombs (1960) proposed the prehnite-pumpellyite metagraywacke facies to include those assemblages produced under conditions of burial metamorphism such as: quartz-prehnite-chlorite or quartz-albite-pumpellyite-chlorite, without zeolites and without characteristic minerals, jadeite or lawsonite, of the glaucophane schist facies. Seki (1961) also proposed pumpellyite-prehnite facies to fill the gap between the zeolite facies and the greenschist facies. Since the work of Coombs (1960) and Seki (1961), reports of prehnite-bearing rocks have been numerous.

Statement of Problem

Since prehnite has been accepted as an index mineral defining the limits of the prehnite-pumpellyite metagraywacke facies (Coombs, 1960), pumpellyite-prehnite facies (Seki, 1961), and pumpellyite-prehnite-quartz facies (Winkler, 1967), it becomes essential to develop an environmental model of its occurrence. This investigation is an attempt to evaluate the temperature and pressure parameters defining the stability of prehnite. It is understood, as the results will show, that the compositional parameter is also of great importance in determining the stability

of prehnite. A work of this type is only the beginning of the data collecting necessary to fully define the conditions under which prehnite forms. The results should not be rigorously applied to geologic occurrences without further knowledge of prehnite and related mineralogical systems.

Previous Experimental Work

Fyfe, Turner, and Verhoogen (1958) presented the first experimental data on the stability of prehnite (Fig. 1). Although a glass of prehnite composition was used in the experimentation, the chemical inequality of prehnite and thomsonite suggests that chemical variation is shown as well as temperature and pressure variations. Anorthite can be converted into thomsonite according to the following equation:

$$CaAl_2Si_2O_8 + 2.4H_2O \rightleftharpoons CaAl_2Si_2O_8 \cdot 2.4H_2O$$

(anorthite) + (water) $\rightleftharpoons$ (thomsonite).

The temperature of the reaction varies with water pressure and ranges slightly above 300°C (Goldsmith, 1952).

Following the work of Fyfe et al. (1958), temperature and pressure diagrams for prehnite and related minerals were developed by Coombs et al. (1959) (Figs. 2 and 3). The stability fields, as outlined, are very indefinite and include compositional variations. It is the purpose of this investigation to refine the stability field of prehnite in a compositionally nonvariant system.

Coombs (1960) combined the above data with the field occurrence of various calcium aluminum silicate minerals in a

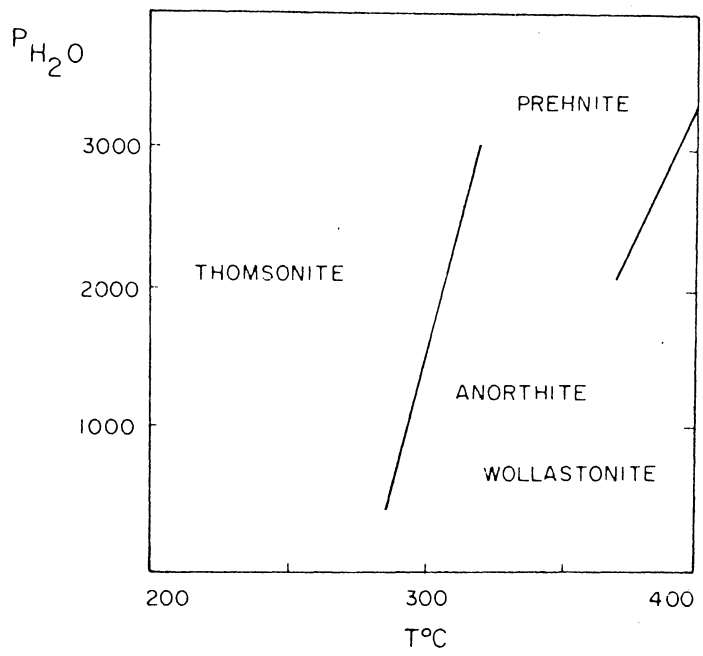

Figure 1. Phases Formed on Crystallization of a Glass of Prehnite Composition--After Fyfe, Turner, and Verhoogen (1958)

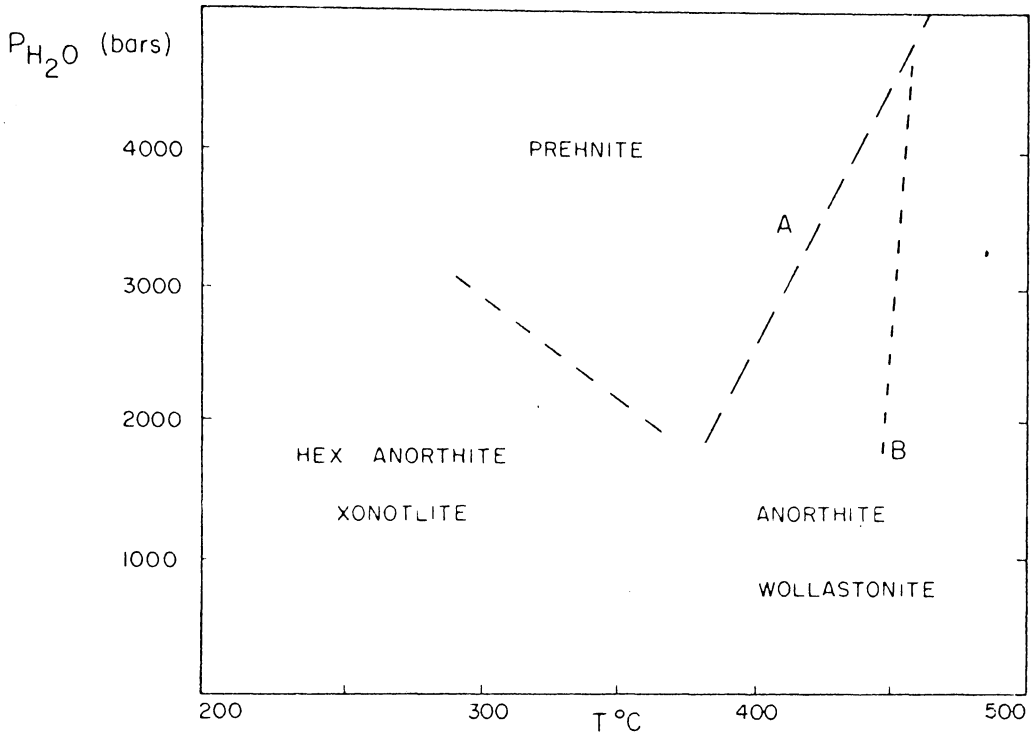

Figure 2. Phases Formed by Crystallization of a Glass of Prehnite Composition--After Coombs et al. (1959).

Line A represents the upper limit of strong prehnite growth. Small amounts of prehnite persist up to line B. Boundary lines represent limits of major fields and changes in assemblages are transitional.

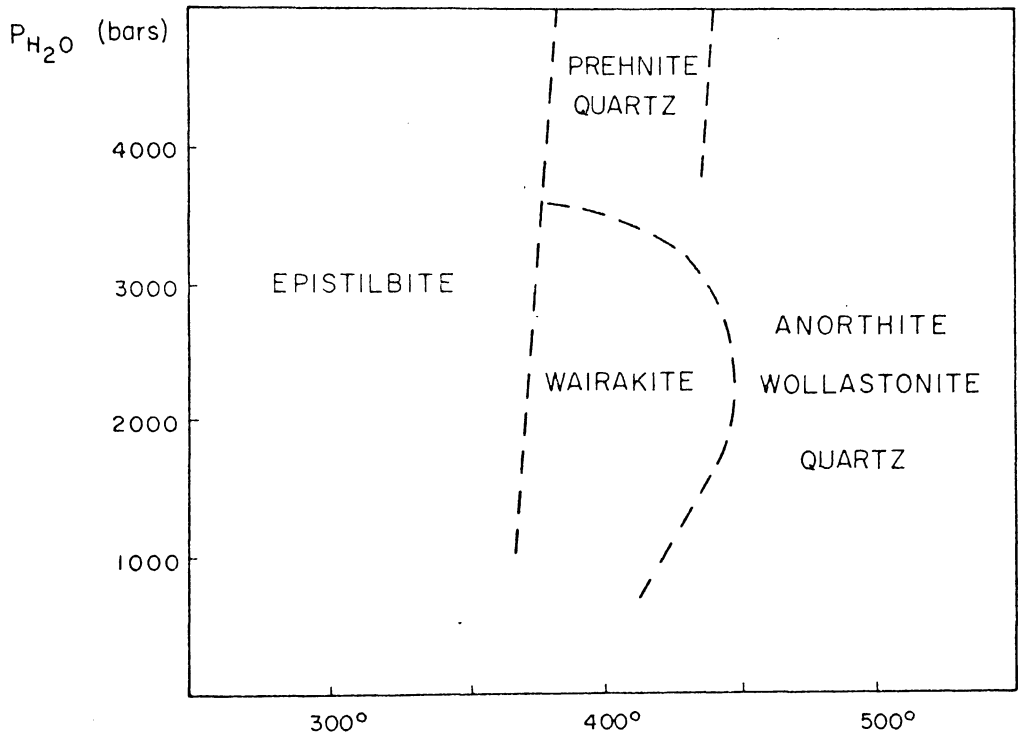

Figure 3. Phases Formed by Crystallization of a Glass of Composition: Prehnite + 4 Silica--After Coombs et al. (1959)

pressure-temperature diagram (Fig. 4) to show the relative stability fields of these minerals. No attempt was made to quantify the temperature and pressure variables, and the composition varies so widely that a direct application to geological problems would seem tenuous. In addition, it is important to consider the stability of prehnite at low water pressures (1-3 kilobars or lower). A study of prehnite stability at these low pressures has considerable geologic application when considering burial metamorphism. The present study should be applicable to these conditions.

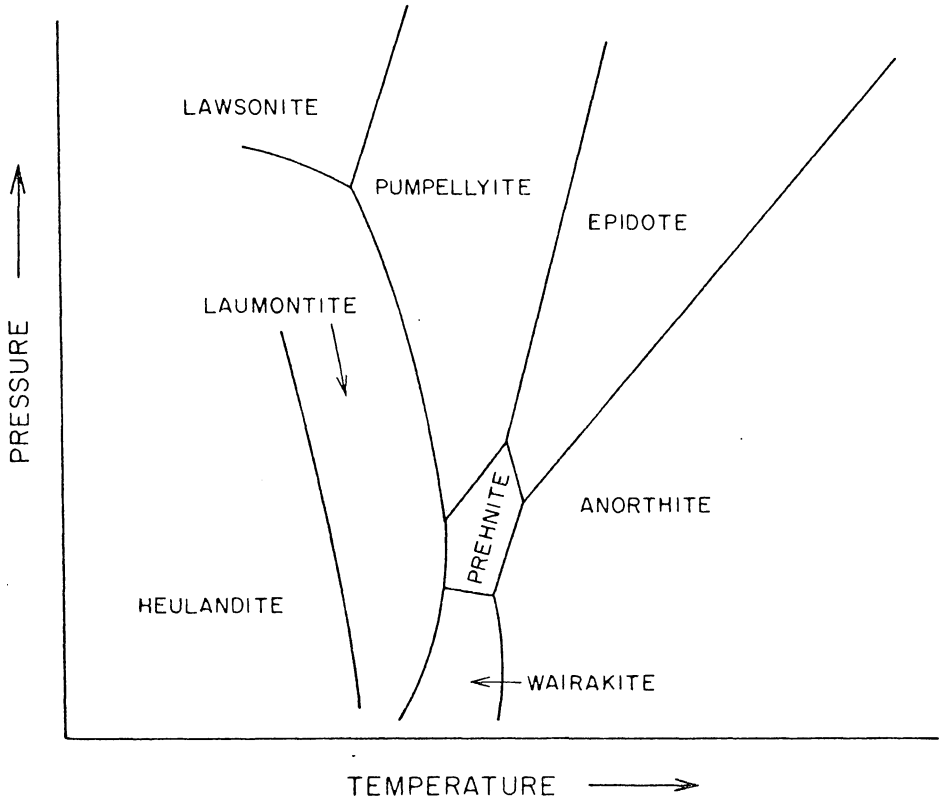

Figure 4. Possible Form of Pressure-temperature Diagram for Assemblages Containing Ca-Al Silicates and Excess Chlorite, Quartz, and Water--After Coombs (1960)

CHAPTER 2

PREHNITE

Prehnite is a sheet silicate which has often been considered to be a zeolite. Though it commonly is associated with the zeolites, the dehydration curve obtained by Gallitelli (1928) shows that there is a loss of 0.2% water at 230°C with the remainder being retained until between 600°C and 700°C. Prehnite cannot be classified with the zeolites because dehydration curves for zeolites show that their water is given off continuously rather than in separate stages at definite temperatures. Another factor eliminating prehnite from the zeolite groups is that all zeolites have an O/Al + Si ratio equal to 2, whereas prehnite has an O/Al + Si ratio of 5/11.

Composition

Natural prehnite occurs with a relatively constant composition and can be ideally described as:

$$Ca_2Al_2Si_3O_{10}(OH)_2.$$

Prehnite does not show any marked variation in its unit cell content; the only significant substitution is iron for aluminum (Fig. 5). As is common in alumino-silicates, some Al appears to enter the Si position and, presumably, Fe''', Fe'', Ti, and Mg substitute into the Al position. Na and K are grouped with the Ca. Neglecting the minor elements, Nuffield (1943) ascertained that a prehnite from Ashcroft, British

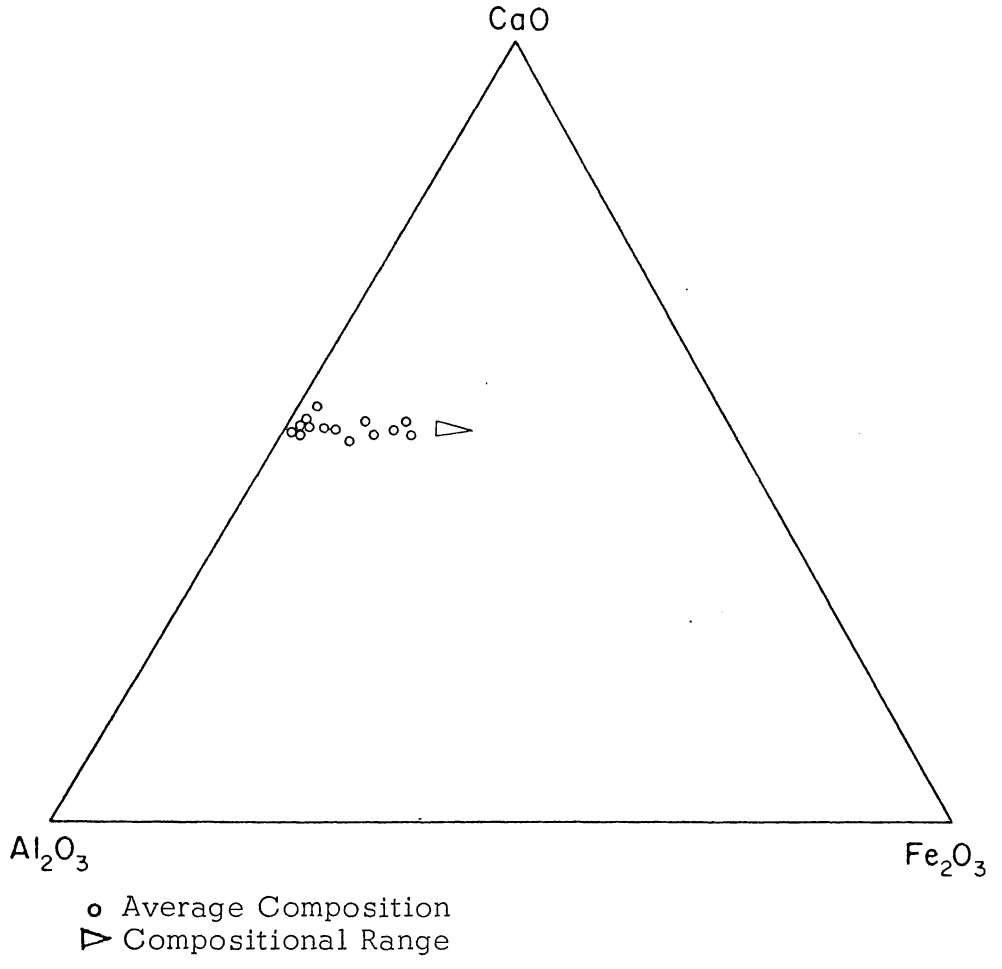

Figure 5. CaO-Al2O3-Fe2O3 Variation Diagram for Prehnite in the Karmutsen Group--After Surdam (1969)

Columbia, has a unit cell content as follows:

$$Ca_{4.06}Al_{3.83}Si_{6.00}O_{19.55}(OH)_{4.04}.$$

This formulation has interesting consequences which will be discussed in detail in Chapter 5.

The chemical analyses listed in Table 1 indicate the rather constant composition. It can also be seen that there is a persistent, yet slight, deficiency in silica and a corresponding excess in alumina. This observation agrees well with the cell content given by Nuffield (1943). Although it may be structurally correct to consider $Ca_2Al_2Si_3O_{10}(OH)_2$ as the theoretical composition, it may be more realistic to consider a composition similar to Nuffield's Ashcroft prehnite.

Structure

Prehnite is an orthorhombic mineral containing two formula weights per unit cell. Gossner and Mussgnug (1931) suggested that the space group is either P2cm or Pncm. Nuffield (1943) reported that single crystal photographs display systematically missing spectral lines, indicative of space group Pncm. However, this space group is not consistent with the pyroelectric character of prehnite (Traube, 1894), and Nuffield concluded that his material is twinned, with untwinned crystals having symmetry P2cm. Peng, Chou, and Tang (1959) also worked on the structure of prehnite and concluded that their material belonged to the space group Pncm. Preisinger (1965) refined the structure of a prehnite from Radautal, Harzburg, and assigned it the space group P2cm.

TABLE 1

PREHNITE: SELECTED ANALYSES

A. From Nuffield, 1943, p. 63-64.

PREHNITE: SELECTED ANALYSES, WITH CELL CONTENTS
OPTICAL PROPERTIES AND SPECIFIC GRAVITIES

	1	2	3	4	5	6	7	A
SiO_2	42.61	42.78	42.79	42.76	42.86	42.38	41.67	42.55
Al_2O_3	23.82	25.37	24.60	24.83	26.55	24.41	24.44	24.86
Fe_2O_3	1.73	0.87	0.60	0.13	0.08	1.20	1.03	0.81
FeO	....	....	1.28	1.12	0.65	....	0.32	0.48
MnO	....	....	....	0.05	trace	....	trace	0.01
MgO	0.13	trace	0.05	0.07	trace	....	0.25	0.07
TiO_2	....	....	....	....	....	....	0.12	0.02
CaO	26.10	26.95	26.52	26.84	25.18	27.90	27.25	26.68
Na_2O	2.09	0.30	....	0.03	....	....	0.18	0.37
K_2O	0.03	trace	....	0.18	....	....	0.18	0.06
H_2O+	3.57	4.18	4.51	4.24	4.86	4.16	4.44	4.27
H_2O-	0.19	....	....	....	....	....	....	0.03
	100.27	100.45	100.35	"100.42"	100.18	99.99	99.88	100.20
Si	5.97	5.89	5.89	5.91	5.83	5.89	5.79	5.88
Al	3.93	4.11	3.99	4.04	4.26	3.99	4.00	4.05
Fe‴	0.18	0.09	0.06	0.01	0.01	0.13	0.11	0.08
Fe″	....	....	0.15	0.13	0.07	....	0.04	0.06
Mn	....	....	....	0.01	....	....	....	0.00
Mg	0.03	....	0.01	0.01	....	....	0.05	0.01
Ti	....	....	....	....	....	....	0.01	0.00
Ca	3.92	3.97	3.91	3.97	3.67	4.15	4.05	3.95
Na	0.57	0.08	....	0.01	....	....	0.02	0.10
K	0.01	....	....	0.03	....	....	0.02	0.01
OH	3.33	3.83	4.14	3.91	4.41	3.80	4.11	3.93
O	20.67	20.17	19.86	20.10	19.60	20.20	19.89	20.07
(Si,Al)	6.00	6.00	6.00	6.00	6.00	6.00	6.00	6.00
(Al,Fe‴,Fe″, Mn,Mg,Ti)	4.11	4.09	4.10	4.13	4.17	4.01	4.00	4.09
(Ca,Na,K)	4.49	4.05	3.91	4.01	3.67	4.15	4.09	4.05
(O,OH)	24.00	24.00	24.00	24.00	24.00	24.00	24.00	24.00
α	1.615	1.612	1.613	1.613	1.619	1.612	1.615	1.614
β	1.627	1.617	1.620	1.620	1.625	1.618	1.624	1.622
γ	1.647	1.644	1.636	1.635	1.643	1.642	1.644	1.642
$2V$	55½°	...	70°	69½°	....	64°	69°	66°
G	....	2.900	2.928	2.928	2.928	....	2.915	2.920

1. Botogol, Eastern Sayan Mountains, Siberia (tabular crystals); anal. Vrevskaya, in Kupletsky (1925). 2. Lake Nipigon, Ont., Canada (cream-yellow radiating globules); anal. Rickaby, in Walker and Parsons (1926). 3. From a skarn at Lísná near Nové Město, western Moravia; anal. Kratochvíl (1932). 4. Near Čáslav, eastern Bohemia (spherulitic, comb-like aggregates); anal. Kratochvíl (1934). 5. Val d'Aosta, Piedmont, Italy; anal. Rondolino (1938). 6. Coopersburg, Berks County, Penn. (light green crystals), aver. of 2 analyses with Fe, Mg, Mn, Cu traces (spectrog.); anal. Wiegner, in Fraser, Butler and Hurlbut (1938). 7. Ashcroft, British Columbia, Canada (colourless crystals); anal. Nuffield (this paper). A. Averages of 1—7.

TABLE 1. Selected Analyses--Continued

B. From Deer et al., 1962, p. 264.

	1.	2.	3.	4.	5.	6.	7.
SiO_2	42·76	44·04	42·86	42·78	43·7	41·67	43·08
TiO_2	—	0·03	0·01	—	tr.	0·12	—
Al_2O_3	24·83	24·77	24·41	25·37	24·05	24·44	24·55
Fe_2O_3	0·13	0·20	0·52	0·87	0·93	1·03	1·40
FeO	1·12	0·00	0·28	—	0·03	0·32	—
MnO	0·05	0·00	0·06	—	0·00	—	0·02
MgO	0·07	0·01	0 03	tr.	0·11	0·25	0·12
CaO	26·84	26·99	26·89	26·95	26·85	27·25	26·65
Na_2O	0·03	0·00	0·32	0·30	0·04	0·18	—
K_2O	0·18	0·00	0 01	tr.	0·00	0·18	0·38
H_2O^+	4·24	4·20	4·45	4·18	4·54	4·44	3·28
H_2O^-	—		0·08	—	0·03	0·00	—
Total	100·25	100·25	99·92	100·45	100·36	99·88	100·52
α	1·613	—	1·613	1·612	1·615	1·615	—
β	1·622	—	1·624	1·617	1·624	1·624	—
γ	1·637	—	1·638	1·614	1·643	1·644	—
$2V_\gamma$	68°50′	—	68°	—	69°	69°	—
D	2·928	—	2·936	2·900	—	2·915	—
NUMBERS OF IONS ON THE BASIS OF 24(O,OH).							
Si	5·909	6·036	5·980	5·884	5·989	5·786	6·043
Al	0·091 → 6·00	—	0·070 → 6·00	0·116 → 6·00	0·011 → 6·00	0·214 → 6·00	—
Al	3·953	4·002	3·900	3·998	3·874	3·786	4·000
Fe^{3+}	0·013	0·021	0·050	0·090	0·096	0·106	0·143
Mg	0·014	0·002	0·003	—	0·022	0·051	0·025
Ti	—	0·003	0·001	—	—	0·013	—
Fe^{2+}	0·130	—	0·033	—	0·003	0·038	—
Mn	0·006 → 4·12	— → 4·03	0·008 → 4·00	— → 4·09	— → 4·00	— → 3·99	— → 4·23
Na	0·008	—	0·081	0·079	0·010	0·050	—
Ca	3·973 → 4·01	3·965	3·973 → 4·06	3·970 → 4·05	3·943 → 3·95	4·055 → 4·14	4·006
K	0·032	—	0·001	—	—	0·032	—
OH	3·903	3·840	4·096	3·830	4·150	4·114	3·070

1. Spherulitic hydrothermal prehnite, amphibolite, Markovice, Čáslav, Bohemia (Kratochvíl, 1934).
2. Brown to flesh-coloured prehnite, zoned pegmatite associated with quartz monzonite cutting magnesian limestones, Crestmore, California (Burnham, 1959). Anal. W. F. Blake (Includes P_2O_5 0·01).
3. White fibrous prehnite, rodingite, Pastoki, Hinduhagh, Pakistan (Bilgrami and Howie, 1960). Anal. R. A. Howie.
4. Cream-yellow radiating prehnite, crevice in Keweenawan traps, Lake Nipigon, Ontario (Walker and Parsons, 1926). Anal. H. C. Rickaby.
5. Translucent, very pale green, botryoidal prehnite, cavities in dolerite, Prospect Quarry, New South Wales (Coombs *et al.*, 1959). Anal. A. M. Taylor and J. A. Ritchie (Includes P_2O_5 0·02, Ag 0·01, Pb 0·01, SnO 0·01).
6. Colourless prehnite crystals, fissure in peridotite, E. side of Bonaparte river, Ashcroft, British Columbia (Nuffield, 1943). Anal. E. W. Nuffield.
7. Prehnite, phlogopite deposit, Emel'dzhak, South Yakutia, Siberia (Galyuk, 1956) (Includes a remainder of 1·04 per cent.)

TABLE 1. Selected Analyses--Continued

C. From Surdam, 1969, p. 261.

TABLE 1. PARTIAL ELECTRON MICROPROBE ANALYSES AND CELL DATA OF PREHNITE, KARMUTSEN GROUP

A. Partial electron microprobe analyses of prehnite, Karmutsen Group

Sample no	1	2	3	4	5	6	7	8
SiO_2	43.5	43.3	43.5	44.2	44.3	43.1	44.6	43.0
CaO	26.1	26.0	25.9	25.3	25.8	26.2	25.6	26.3
Al_2O_3	22.6	23.2	24.5	24.4	24.4	25.0	17.4	17.6
Fe_2O_3 (total Fe)	2.6	2.0	0.9	1.1	0.9	0.4	8.0	7.6
Range of Fe_2O_3	0.4 6.8	0.6-10.8	0.5-1.6	0.1-1.4	0.1 5.5	0.1 1.2	4.4 10.3	0.4 9.2
Subtotal	94.8	94.5	94.8	95.0	95.4	94.7	95.6	94.5

B. Prehnite cell data, Karmutsen Group

a Å[a]	4.63	4.63	4.63	4.62	4.62	4.63	4.64	4.64
b Å[a]	5.48	5.58	5.48	5.47	5.49	5.49	5.49	5.49
c Å[a]	18.5	18.5	18.5	18.5	18.5	18.5	18.5	18.5
V (Å^3)[b]	470	469	468	467	469	470	472	471

[a] (±0.003)
[b] (±0.2)

Papike and Zoltai (1967) examined crystals from various localities and concluded that the average structure has a space group very nearly described by the space group P2cm. The most detailed, and apparently the most accurate, determination of the prehnite structure is that of Papike and Zoltai (1967) shown along the "b" axis projection in Figure 6.

A discussion of the position of aluminum within the structure sheds light on the problem of understanding the space group. Based on interatomic distances, Smith and Bailey (1963) conclude that it is reasonable to assume that the two tetrahedral aluminum atoms are confined to the T_2 positions shown in Figure 6. Papike and Zoltai (1967) show that there are three symmetrically distinct ways of ordering the two tetrahedral aluminum atoms over the four T_2 positions. All three ways lead to a reduction of the Pncm space group symmetry; these are illustrated in Figure 7. Ordering scheme (A) leads to a space group P2cm, ordering scheme (B) leads to a monoclinic symmetry P2/n, and ordering scheme (C) results in space group $P22_12$. $P22_12$ does not appear to be feasible since it leads to Al-O-Al linkages which are unstable in silicates (Lowenstein, 1954). Papike and Zoltai (1967) also observed that many prehnites had a $P222_1$ space group. This leads to some confusion since $P222_1$ is not a subgroup of Pncm, and thus the structure could not be refined in this space group. Okl precession photographs of several prehnites indicate that the apparent $P222_1$ space group results from two phases being intimately intergrown in the prehnite structure, one monoclinic and the other orthorhombic (Papike and Zoltai, 1967). If this is true, the reflections violating the "c" glide plane could be due to a twinned P2/n phase.

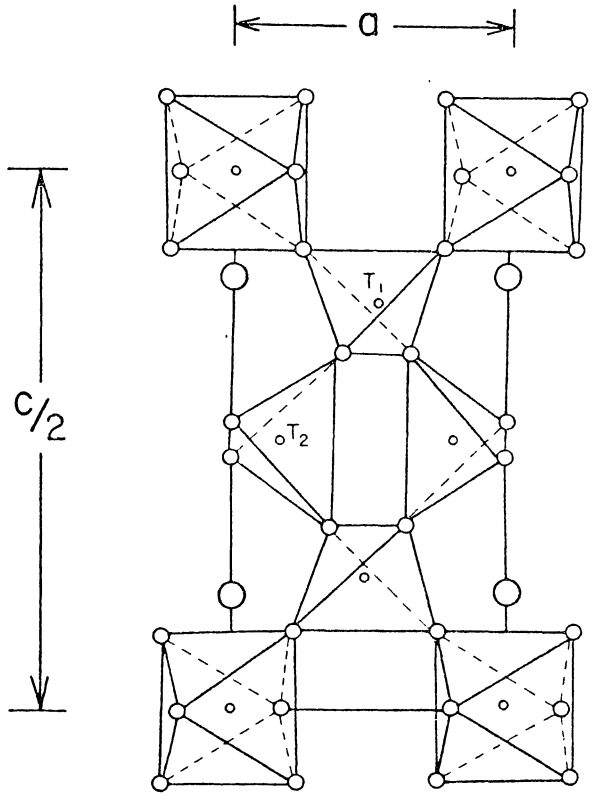

Figure 6. Structure of Prehnite

The diagram is one-half unit cell projected along the "b" axis of the crystal structure--After Papike and Zoltai (1967).

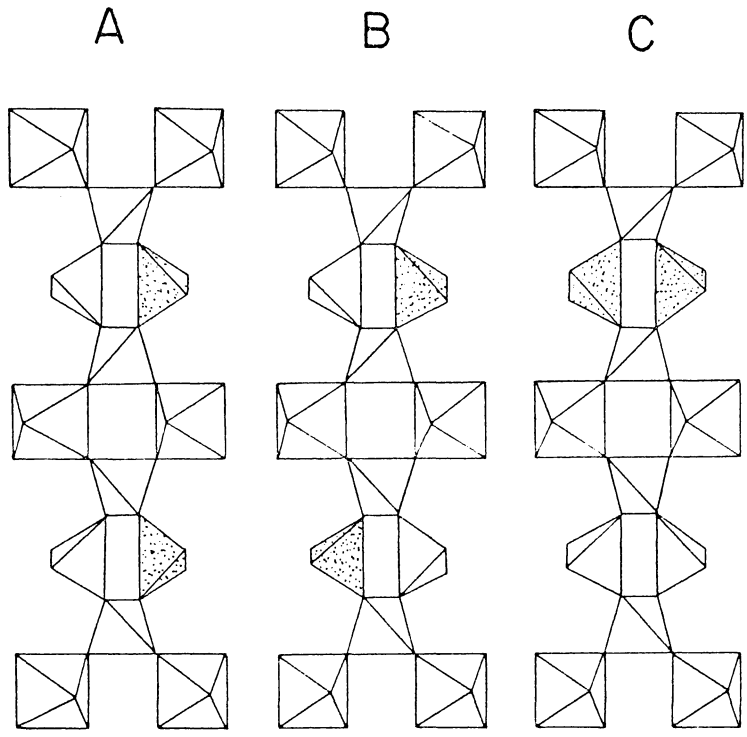

Figure 7. Tetrahedral Aluminum Ordering

Three ordering schemes determined by Papike and Zoltai (1967) for tetrahedral aluminum in prehnite. Shaded tetrahedra contain aluminum.

The occurrence of intimate intergrowths of twinned monoclinic and orthorhombic domains might explain some of the peculiar optical properties exhibited by prehnite. In crystals composed of both monoclinic and orthorhombic domains, the basic structure would be continuous, but the ordering scheme for the tetrahedral aluminum would change. The following interpretations (Papike and Zoltai, 1967) are possible for prehnites with these apparent symmetries:

Pncm	disordered prehnite
P2cm	crystals composed mainly of ordering scheme A
P2/n	crystals composed mainly of ordering scheme B
$P22_12$	crystals composed mainly of ordering scheme C, which would be highly unlikely.
$P222_1$	crystals composed mainly of domains of both P2cm and P2/n symmetries.

The P2cm and P2/n polymorphs should have very similar free energies, because crystals are commonly composed of intimate intergrowths of both polymorphs, and different crystals from the same locality show varying proportions of the two polymorphs. Although prehnites have an average structure with symmetry very nearly described in space group Pncm, most crystals have an ordered distribution of tetrahedral aluminum leading to crystals with symmetries P2cm or P2/n. Crystals studied from several localities appear to be composed of both P2cm and P2/n domains. These complications explain the confusion during early investigations concerning the space group of prehnite.

Optical and Physical Properties

The optic axial plane is parallel to (010) and thus perpendicular to the (001) cleavage plane. The optic angle ($2V_{\gamma}$) ranges from approximately 65 degrees to 69 degrees. Deer, Howie, and Zussman (1962) list the refractive indices as: α (1.611–1.632), β (1.615–1.642), and γ(1.632–1.665). The refractive indices for the Patterson, New Jersey, sample used in this study was determined to be α1.614, β1.624, and γ1.644. The birefrigence can vary from 0.022 to 0.035, and for the Patterson, New Jersey, sample it is 0.029. Nuffield (1943) found no evidence that variations in the amounts of Fe_2O_3 or (OH) had any effect on the values of the refractive indices. However, Deer et al. (1962) state that the refractive indices and birefringence increase with increasing amounts of iron. Extinction is parallel to the cleavage traces, though it is often wavy and sometimes incomplete. This may be the result of intimate intergrowths of the monoclinic and orthorhombic domains.

Distinct individual crystals of prehnite are rare. Tabular groups, barrel-shaped aggregates, and reniform globular masses are more common, often giving the characteristic "bow tie" appearance (Deer et al, 1962). This "bow tie" appearance is due to the occurrence of crystal segments in three different orientations: (1) segments in a plane parallel to [001] ; (2) segments normal to the [001] plane, in which the crystals are composed of layers rotated 90 degrees to each others; and (3) segments in a medial band with simple orthorhombic orientation (Richmond, 1938).

The density varies from 2.90 gm/cm^3 to 2.95 gm/cm^3 with a corresponding variation in molar volume from 142.05 cm^3 to 137.86 cm^3.

The density variation is a result of the varying amounts of iron substituting for aluminum in the structure; an increase in the iron content increases the density. The iron content is also responsible for the color of hand specimens. Iron-poor prehnite is colorless to flesh colored, while iron-rich prehnite is pale green. The prehnite used in this investigation, from Patterson, New Jersey, is pale green, indicating the presence of some iron in the structure. In hand specimen, the Patterson prehnite has a botryoidal texture and is intimately intergrown with calcite ($CaCO_3$) and stilbite ($CaAl_2Si_2O_{18} \cdot 7H_2O$).

Occurrence

Prehnite is not a common mineral, but it is interesting and important in view of its wide variety of occurrences. It occurs chiefly in basic igneous rocks as a secondary or hydrothermal mineral in veins, cavities, and amygdales (Deer et al., 1962). It is frequently associated with zeolites. Kerr (1959) comments on "magnificent" specimens of prehnite occurring in amygdales at Patterson, New Jersey; samples from this locality have been used in this investigation. Prehnitized amygdaloid basalts were found in a collection of glacial boulders at Hasau, Courland and East Prussia (Eskola, 1934). Fraser, Butler, and Hurlbut (1938) and Simpson (1969) have noted prehnite occurring in veinlike bodies cutting Triassic diabase near Coopersburg, Pennsylvania.

Prehnite is also found in veins in granites, diorites, and monzonites. Occurrences of this type have been reported by Baker (1953), Richmond (1938), Kupletsky (1925), and Burnham (1959). Such occurrences are often considered to be micropegmatites which are associated with the intrusion of acidic igneous rock into limestone. A typical

example of this is the Botogol Massif. Here, syenites and nepheline-syenites have been enriched in calcium and have been converted to diorites. The prehnite veins are developed in the contact diorite where calcium metasomatism has taken place (Kupletsky, 1925).

In metamorphic rocks it is found in contact-altered, impure limestones and marls, and in rocks in which calcium metasomatism has occurred, such as those described above. Taylor (1935) describes a prehnite found in a zone of "dark" silicates in contact rocks from the Little Belt Mountains, Montana. By far the most widely reported occurrence of prehnite is in regional metamorphic rocks. It may be formed from the alteration of calcium-rich feldspars or from calcium-poor feldspars, if calcium metasomatism has operated on the system. Occurrences of this type have been reported by Coombs (1954), Coombs et al. (1959), Watters (1964), and Watson (1953). Coombs et al. (1959) state that prehnite is stable in the greenschist and zeolite facies, whereas Winkler (1967) and Turner (1968) restrict prehnite to metamorphic grades below the greenschist facies.

One unusual occurrence has been noted by Hall (1964). This prehnite is closely associated with biotite; lenticular layers of prehnite are intergrown in large biotite crystals. A possible explanation of this occurrence is that the biotite and prehnite formed simultaneously from hornblende as a result of low temperature potassium metasomatism (Hall, 1964). Natural prehnite is known to be closely associated with the following minerals: calcite, stilbite, pumpellyite, quartz, anorthite, biotite, chlorite, sericite, datolite, laumontite, titaniferous augite, sphene, zeolites, albite, oligoclase, and microcline.

The potential value of this investigation is reflected in the wide variety of geologic environments in which prehnite occurs. This work will give some insight into the conditions under which prehnite can occur. A further importance stems from the fact that Winkler (1967) and Turner (1968) have included prehnite as an index mineral in defining metamorphic grades below the greenschist facies. This status as an index mineral enhances the importance of determining the conditions under which prehnite is stable.

CHAPTER 3

EXPERIMENTAL PROCEDURES

This study is the first experimental study to be completed in the Laboratory of Experimental petrology at The University of Arizona. It was, therefore, necessary to develop much of the apparatus and techniques. The three primary areas of consideration were: (1) the proper preparation of the sample; (2) control of the experimental conditions; and (3) accurate analyses of the results of experimentation.

Sample Preparation

Both naturally occurring prehnite and gels of prehnite composition were used in this investigation. However, the major portion of the starting material was naturally occurring prehnite from Patterson, New Jersey. The material is from amygdaloidal fillings in an altered diabase. Figure 8 is a photomicrograph showing the prehnite in contact with the diabase. The radiating crystals seen in this figure develop a classic example of a botryoidal surface in the center portion of the amygdale. The prehnite is intimately associated with calcite; However, it is not known whether they were formed simultaneously or formed individually under the influence of a delicate balance of conditions. Stilbite is also associated with the prehnite but is apparently a later phase.

The material was carefully crushed into fragments approximately one centimeter in diameter. These fragments were sorted in an effort to obtain the least contaminated sample; fragments containing

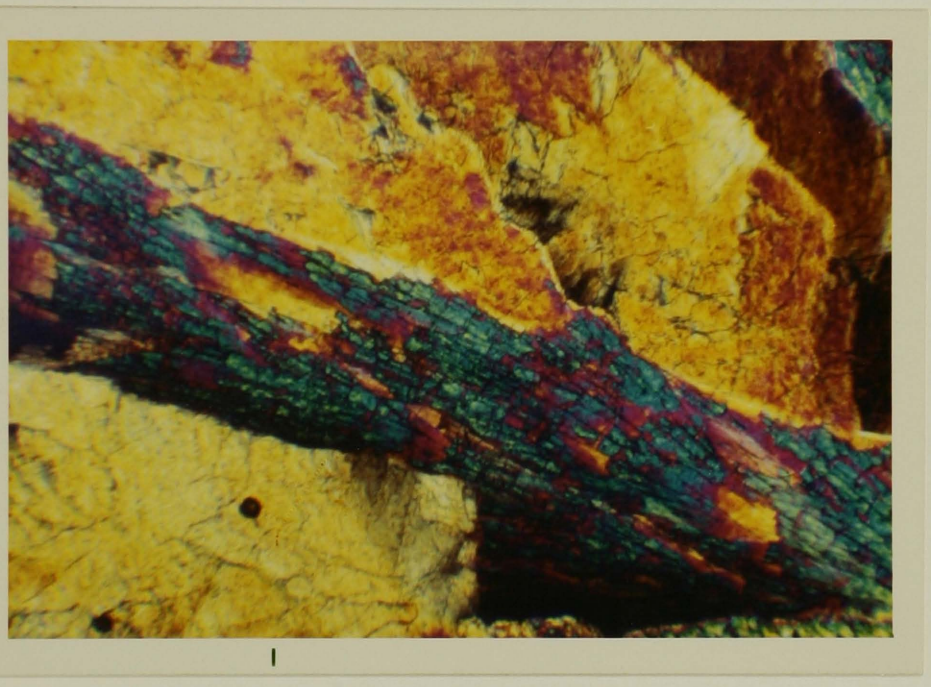

Figure 8. Photomicrograph of the Patterson, New Jersey Prehnite

macroscopically visible calcite were rejected. The fragments chosen were then leached in hydrochloric acid to dissolve any remaining calcite present on the surface. The material was then crushed in a percussion-type iron mortar and pestle and sieved through one millimeter and 60 mesh sieves. Material less than 60 mesh was discarded. The material contained in the 60 mesh was then microscopically analyzed, and any grain of questionable composition was rejected. The one millimeter sieve produced a grain size that could be easily observed microscopically, but one that was not easily ground in the agate mortar and pestle. Though initial grinding in the agate mortar and pestle was difficult, further crushing in the iron mortar and pestle was avoided to eliminate possible contamination. Grinding in the agate mortar and pestle was continued until further grinding produced no appreciable change in the grain size. Due to the hardness of the material, it was particularly difficult to reduce the prehnite to an adequately small grain size. These precautions produced a starting material of very high purity.

As a further test of the quality of sample preparation, the prehnite was prepared in several lots. Samples from different lots were exposed to the same experimental conditions and there were no observable differences in the resulting products.

These techniques used in gel preparation are outlined by Luth and Ingamells (1965). The source materials of the various oxides are as follows:

Oxide	Source
CaO	Calcite ($CaCO_3$)
Al_2O_3	$Al(NO_3)_3 \cdot 9H_2O$
SiO_2	Ludox

Ludox is a trade name of the E. I. du Pont de Nemours Company and is an ammonia stabilitized silica solution of high purity. Known amounts of calcite and $Al(NO_3)_3 \cdot 9H_2O$ were dissolved in nitric acid, care being taken not to supersaturate any of the solutions. The source solutions were combined in the desired proportions to achieve the necessary compositions. The gel was then evaporated to dryness and heated with a Bunsen burner to drive off the excess NO_2. The gels were used to help substantiate the prehnite dissociation curve and to determine the true composition of the Patterson, New Jersey, prehnite.

Experimental Apparatus and Methods

Cold seal stellite pressure vessels (Tuttle, 1949) were employed for all experimental runs. Figure 9 is a diagrammatical representation of a vessel. The purpose of the research was to evaluate the stability of prehnite under geologically important conditions, i.e., less than 3 kilobars water pressure. The pressure-temperature range of these vessels adequately covers these conditions. The particular cold seal vessels used were produced by Tem-Press Research.

Pressure is applied to the system with a S-440 Hydraulic Power Unit manufactured by Sprague Engineering. The unit provides fluid output pressures to 30,000 psi and can be adapted to pump oil, water, or inert chemicals. To obtain pressures greater than 20,000 psi, the

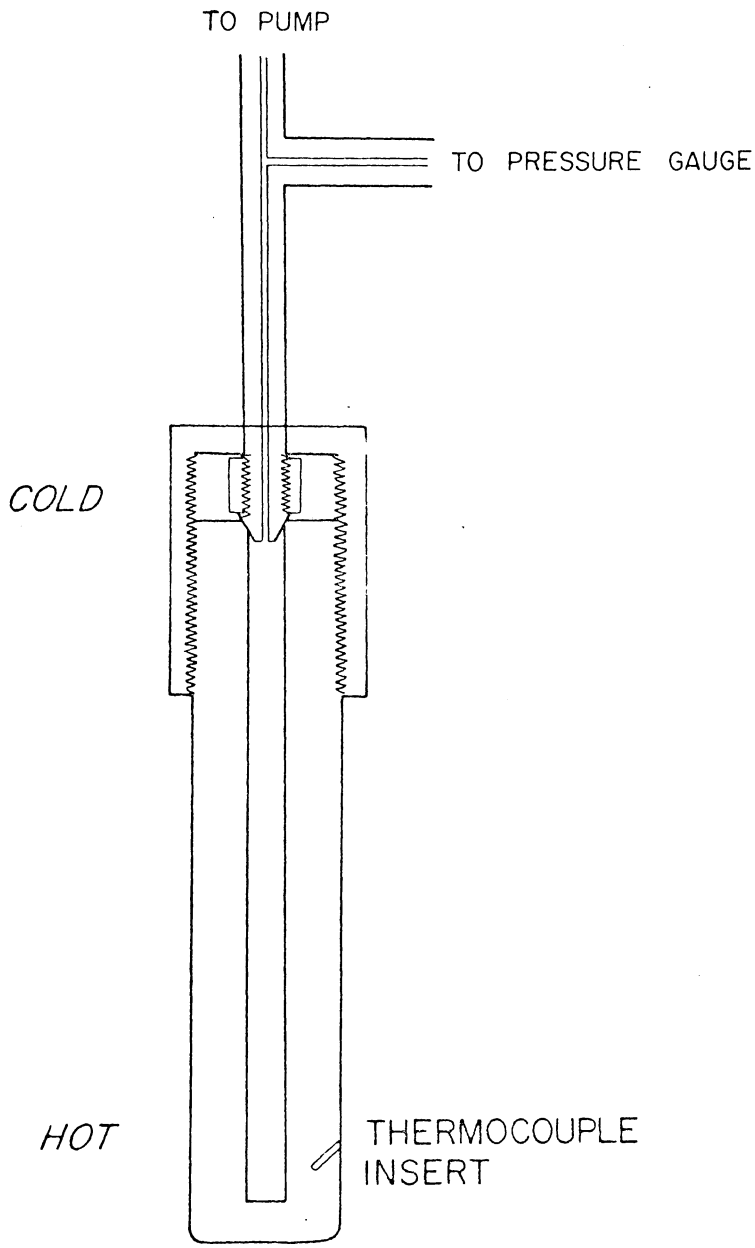

Figure 9. Cold Seal Pressure Vessel--After Tuttle (1949)

hydraulic power unit is used to produce the first 20,000 psi. The system is then closed. From this point increasing temperature could easily bring the system to a pressure greater than 45,000 psi. With this method it is necessary to bleed off excess pressure by operating the hand valve. At pressures less than 20,000 psi the hydraulic power unit can be used to maintain the proper pressure as the temperature equilibrates. This is accomplished by using the pump to automatically bleed off excess pressure. The unit operates on 40 psi water pressure, which is standard for normal water supplies, and up to 100 psi air pressure.

The pressure gauges are of the Bourdon type and were also obtained from Tem-Press Research. The gauge was calibrated and checked to 1/4 percent accuracy of full range before shipment.

The temperature controlling devices are Model 152P Amplitrols manufactured by Wheelco Instruments Division of Barber-Coleman Company. Model 152P is an "anticipatory" time proportioning controller which compensates for system inertia. The "anticipatory" action starts as soon as the controller temperature comes within the proportioning band of the instrument, i.e., 1 percent of scale range to either side of the control point. Twenty-four gauge chromel and alumel wire was used for this temperature sensing device.

The furnaces were constructed and designed by Dr. Bert Nordlie, John Delaney, and the author. The furnace shells are constructed of nine-inch lengths of transite pipe which is eight inches in diameter. Standard nichrome split heating elements are mounted vertically and packed in Johns-Manville insulation bricks and shredded No. 352 asbestos. When operating at a temperature of 650^{o}C, the

exterior of the furnace is cool enough to touch. These ovens are efficient and can maintain pressure vessel temperatures to within $\pm 2^{o}C$.

The temperature of the hydrothermal vessel is monitored with a second chromel-alumel thermocouple and recorded on a Leeds and Northrup No. 7656 portable double range millivolt indicator. The potentiometer has a maximum error of 1 and 1/2 percent at $1000^{o}C$. Considering all errors within the heating system, the temperatures are accurate to at least $\pm 5^{o}C$.

Quenching of the experimental charges is accomplished by immersing the hot portion of the pressure vessel in water at room temperature. This procedure made it possible to remove the sample from the pressure vessel within five minutes. Considering the slow reaction rates observed, this was more than sufficient. Reaction rates will be more fully discussed in Chapter 4.

All samples used for the determination of the stability fields contained 20 percent by weight water. Distilled water was used for this purpose so that no impurities would be introduced. The proper weights were obtained by using a Mettler H20T balance with an error factor of ± 0.00005 grams. First, the water was loaded into the capsule with a Hamilton Microlitre No. 701, and then the proper weight of prehnite was added. The samples usually contained 10 to 15 milligrams of prehnite; this amount was adequate fro both optical and X-ray analyses.

The samples were sealed in either 2.0 mm O.D. or 2.5 O.D. gold capsules. Confident and quick welding is necessary to insure that the volatiles are not lost in the sealing process. There are several tests which indicate whether the sealing process is successful or not.

Comparison of the capsule weight before and after sealing can be used to determine if the volatiles have been lost. This test is valid if the amount of gold vaporized during the welding process is negligible. If there is a loss of weight, it can be assumed that a comparable amount of volatiles has been lost. If the capsule completely collapses upon pressurization it indicates no leaks in the seal. Proper sealing is also indicated if the weight of the capsule remains the same after the experimental run. If leakage occurs during the course of the run, the capsule may gain weight because the capsule does not completely collapse and water is allowed to enter. The continued presence of the volatile phase can also be shown by pressure quenching at low temperatures. If water is in the gaseous state, the elevated temperature causes swelling of the capsule. Similarly, pressure quenching at elevated temperatures causes the capsules to rupture, indicating continued presence of the volatiles.

Methods of Sample Identification

The primary tool for sample identification is the petrographic microscope. The crystalline products grown attain a size sufficient to allow optical determination once a positive identification of the phases is obtained. A Phillips X-ray diffractometer is used to positively identify all phases concerned. X-ray analyses of samples close to the dissociation curve, yet in the prehnite field, showed no sign of decomposition. It was, therefore, concluded that optical identification was sufficient. All petrographic identifications were made on the basis of refractive indices. A 1.64 immersion oil blanks out wollastonite and prehnite and allows the identification of anorthite. A 1.58 immersion oil

blanks out anorthite and crystal habit allows easy differentiation between prehnite and wollastonite. In all samples grossularite was easily identifiable from its crystal habit and high indices of refraction.

CHAPTER 4

EXPERIMENTAL RESULTS

Upon decomposition, prehnite formed three crystalline phases: wollastonite, anorthite, and grossularite. The study results defined a univariant curve for the decomposition of prehnite. Thermodynamic extrapolation was necessary at low pressures because kinetic factors inhibited the reaction.

Pertinent Crystalline Phases

The crystalline phases encountered in this investigation were prehnite, anorthite, wollastonite, and grossaluratie. Anorthite and wollastonite form as products from the decomposition of prehnite by the following reaction:

$$Ca_2Al_2Si_3O_{10}(OH)_2 \rightleftharpoons CaAl_2Si_2O_8 + CaSiO_3 + H_2O.$$

Grossularite also forms as a product of the decomposition of prehnite at elevated temperatures, but the mechanism of its origin, which will be discussed later, is not entirely clear. The compositions of all phases in the system $CaO-Al_2O_3-SiO_2-H_2O$. The anhydrous base of this four component system is shown in Figure 10.

Identification of the phases is based on both optical and X-ray analyses. After X-ray analyses had verified optical identification, optical analyses were quite sufficient for identification, since all phases developed optically identifiable crystals.

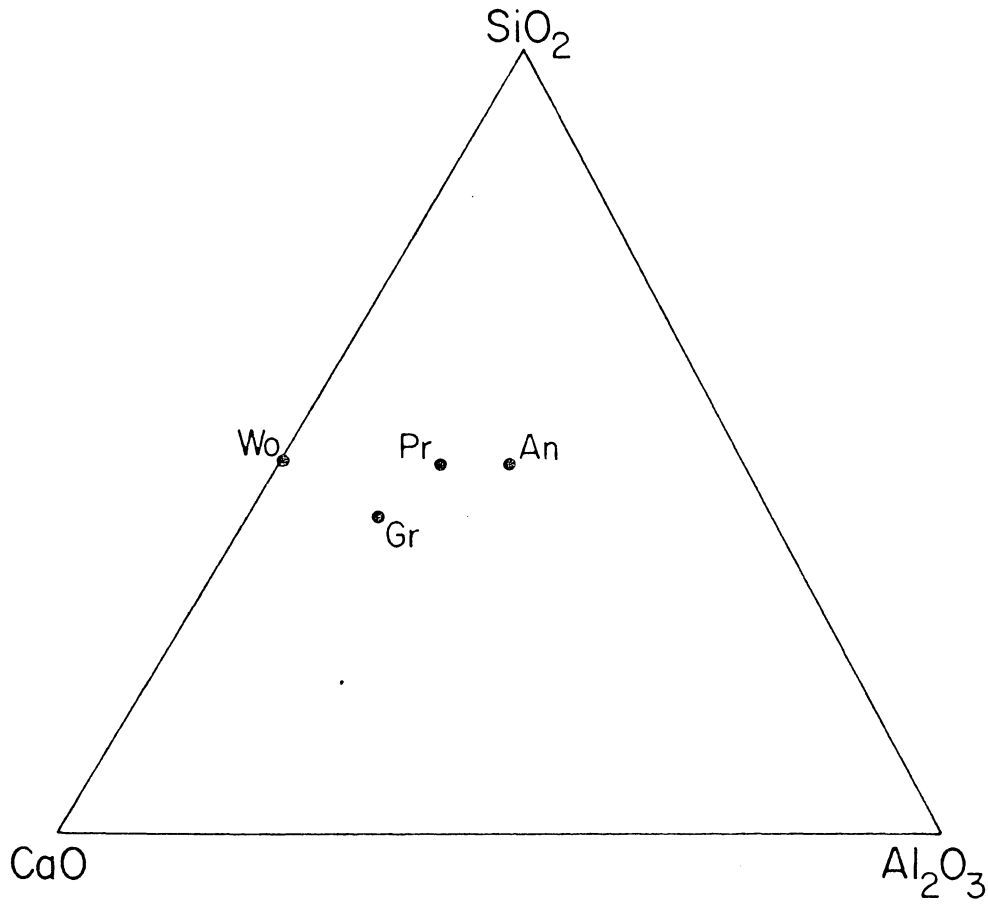

Pr	- Prehnite	$Ca_2Al_2Si_3O_{10}(OH)_2$
An	- Anorthite	$CaAl_2Si_2O_8$
Wo	- Wollastonite	$CaSiO_3$
Gr	- Grossularite	$Ca_3Al_2Si_3O_{12}$

Figure 10. Composition of Pertinent Phases

The anhydrous base of the system $CaO-Al_2O_3-SiO_2-H_2O$ shown with the composition of prehnite projected onto the $CaO-Al_2O_3-SiO_2$ composition plane. Stoichiometric chemical formulae for the phases shown above.

Anorthite, $CaAl_2Si_2O_8$, coexists in equilibrium with wollastonite and grossularite above the temperature at which prehnite decomposes. Anorthite is generally observable optically as laths or as grains with indefinite shapes; it is differentiated from the other phases on the basis of its refractive indices.

Wollastonite, $CaSiO_3$, forms bladed crystals, needles, and radiating groups of needles and blades. Positive identification is obtained by X-ray diffraction, although it is generally easy to identify optically. The ease of identification is enhanced by large crystal growth and diagnostic crystal shapes. The crystal habit makes it impossible to determine all of the principal indices; the range of refractive indices is approximately 1.63-1.64.

Grossularite, $Ca_3Al_2Si_3O_{12}$, is by far the easiest phase to identify, yet the most perplexing to understand. It is readily identifiable optically because of its high index of refraction and isotropic nature which are diagnostic. The index of refraction is approximately 1.74. It forms tiny equant crystals with dodecahedral faces. These faces can be observed by moving the petrographic microscope stage up and down. The X-ray diffraction pattern is diagnostic and shows that it is nearly stoichiometric grossularite and not an intermediate member of the solid solution series, grossularite-hydrogrossularite ($Ca_3Al_2Si_3O_{12}$—$Ca_3Al_2(OH)_{12}$). This conclusion is based on the fact that X-ray diffraction patterns of the experimental product identically match previously determined grossularite patterns. Hydrogrossularite and intermediate members of the grossularite-hydrogrossularite series have X-ray diffraction patterns which differ considerably from that of grossularite.

It is therefore concluded that the garnet is grossularite rather than hydrogrossularite.

Experimental Data

All significant experimental runs made during the course of the investigation are listed in Table 2. The data in the table include the physical conditions and the products of the run as follows: the temperatures are given in degrees centigrade and the pressures are given in both bars and pounds per square inch (psi); the runs are listed in chronological order; in the "Remarks" column, K indicates a loss of pressure during the course of the run, R indicates runs used as reversible criteria, and M indicates runs in which prehnite reaction was incomplete. The duration of the run is given in days (d).

Prehnite Stability

The temperature and pressure conditions under which prehnite dissociated are given in Figure 11. The stoichiometric equation for this reaction is as follows:

$$Ca_2Al_2Si_3O_{10}(OH)_2 \rightleftharpoons CaAl_2Si_2O_8 + CaSiO_3 + H_2O.$$

Below 12,000 psi water pressure the reaction rates were slow to immeasurable. Above 12,000 psi water pressure appreciable reaction took place to within 10°C to 20°C of the dissociation curve.

At temperatures of 100°C or more above the dissociation curve the crystallization of the products is rapid, as a consequence of the formation of numerous nuclei and consequently small crystals. At temperatures and pressures closer to the curve fewer nuclei form and larger

TABLE 2

EXPERIMENTAL DATA

Run #	Starting Material	Water Pressure (bars)	Water Pressure (psi)	Temp. (°C)	Duration of Run	Products	Remarks
P-1	prehnite	811	13400	802	7 d	Wo, An, Gr	K
P-2	prehnite	993	14600	703	3 d	Wo, An, Gr	M
P-3	prehnite						control failure bomb blew
P-4	prehnite	1007	14800	606	7 d	Wo, An, Gr	
P-5	prehnite	1013	14880	505	7 d	Wo, An, Gr	M
P-6	prehnite	1082	15900	408	7 d	no reaction	
P-7	prehnite	1040	15300	406	14 d	no reaction	
P-8	prehnite	3000-zero		500	9 d	Gr	
P-9	prehnite	1088	15800	494	14 d	Wo, An, Gr	M
P-10	prehnite dry	1014	14900	395	14 d	Gr	
P-11	prehnite	1014	14900	395	14 d	Gr	
P-12	prehnite	1040	15300	455	9 d	Gr	

TABLE 2. Experimental Data--Continued

Run #	Starting Material	Water Pressure (bars)	Water Pressure (psi)	Temp. (°C)	Duration of Run	Products	Remarks
P-13	prehnite	1040	15300	455	9 d	Gr	
P-14	prehnite dry	1034	15200	591	6 d	Wo, An, Gr	
P-15	prehnite 10% H_2O	1034	15200	591	6 d	Wo, An, Gr	M
P-16	prehnite 50% H_2O	1034	15200	591	6 d	Wo, An, Gr	M
P-17	prehnite	408	6000	410	8 d	Wo, Gr	M, K
P-18	prehnite	408	6000	410	8 d	no reaction	Lost water
P-19	prehnite	1156	17000	475	7 d	Gr	
P-20	prehnite	1156	17000	475	7 d	Gr	
P-21	prehnite	2190	32200	598	7 d	Wo, An, Gr	
P-22	prehnite	557	8200	448	11 d	no reaction	
P-23	prehnite	2244	33000	533	4 d	An, Gr	Not long enough
P-24	prehnite	530	7800	478	7 d	no reaction	Kinetics?

TABLE 2. Experimental Data--Continued

Run #	Starting Material	Water Pressure (bars)	Water Pressure (psi)	Temp. (°C)	Duration of Run	Products	Remarks
P-25	prehnite	2122	31200	568	7 d	Wo, An, Gr	
P-26	prehnite	2394	35200	525	7 d	Gr	
P-27	prehnite	530	7800	478	7 d	no reaction	Kinetics?
P-28	prehnite	530	7800	478	7 d	no reaction	Kinetics?
P-29	prehnite	2190	32200	570	7 d	Wo, An, Gr	
P-30	prehnite	2190	32200	570	7 d	Wo, An, Gr	
P-31	prehnite	3100-zero		572	1.5 d	no data	
P-32	prehnite	530	7800	497	7 d	An, Gr	M
P-33	prehnite	530	7800	497	7 d	An, Gr	M
P-34	prehnite	921	13550	742	2.5 d	Wo, An, Gr	Acid leached
P-35	prehnite	2115-1972		499	11 d	Gr	
P-36	prehnite	2115-1972		499	11 d	100% Gr	Capsule leak

TABLE 2. Experimental Data--Continued

Run #	Starting Material	Water Pressure (bars)	Water Pressure (psi)	Temp. (°C)	Duration of Run	Products	Remarks
P-37	prehnite	921	13550	742	2.5 d	Wo, An, Gr	M
P-38	prehnite	883	13000	489	8 d	Wo, An, Gr	M
P-39	prehnite	883	13000	489	8 d	Wo, An, Gr	M
P-40	prehnite calcite	1088	16000	704	8 d	100% Gr	
P-41	prehnite	1088	16000	704	8 d	Wo, An, Gr	Acid leached
P-42	prehnite	1088	16000	704	8 d	Wo, An, Gr	
P-43	prehnite	823	12100	454	13 d	Gr	
P-44	prehnite	823	12100	454	13 d	Gr	
P-45	prehnite	2040-1435		542	3.5 d	Wo, An, Gr	M, K
P-46	prehnite	2040-1435		542	3.5 d	Wo, An, Gr	M, K
P-47	prehnite	2068	30400	541	14 d	Wo, An, Gr	
P-48	prehnite	2068	30400	541	14 d	Wo, An, Gr	
P-49	prehnite	1877	12900	474	14 d	Gr	

TABLE 2. Experimental Data--Continued

Run #	Starting Material	Water Pressure (bars)	Water Pressure (psi)	Temp. (°C)	Duration of Run	Products	Remarks
P-50	prehnite	1877	12900	474	14 d	Gr	
P-51	prehnite	3108	45700	563	14 d	Wo, An, Gr	
P-52	prehnite calcite	3108	45700	563	14 d	100% Gr	
P-53	prehnite calcite	530	7800	473	14 d	Gr	M
P-54	prehnite	530	7800	473	14 d	Wo, Gr	M
P-55	prehnite	3010	44100	397	14 d	Gr	
P-56	prehnite calcite	3010	44100	397	14 d	Gr	
P-57	prehnite	3115	45800	405	27 d	Gr	
P-58	prehnite calcite	3115	45800	405	27 d	100% Gr	M
P-59	gel	2190	3220	525	14 d	Wo, An	
P-60	prehnite	2190	32200	525	14 d	Gr, Wo, An	

TABLE 2. Experimental Data--Continued

Run #	Starting Material	Water Pressure (bars)	Water Pressure (psi)	Temp. (°C)	Duration of Run	Products	Remarks
P-61	gel	3102	45600	543	14 d	Wo, An	
P-62	gel calcite	3054	44900	538	27 d	Gr	
P-63	gel quartz	3054	44900	538	27 d	Wo, An, Qtz	

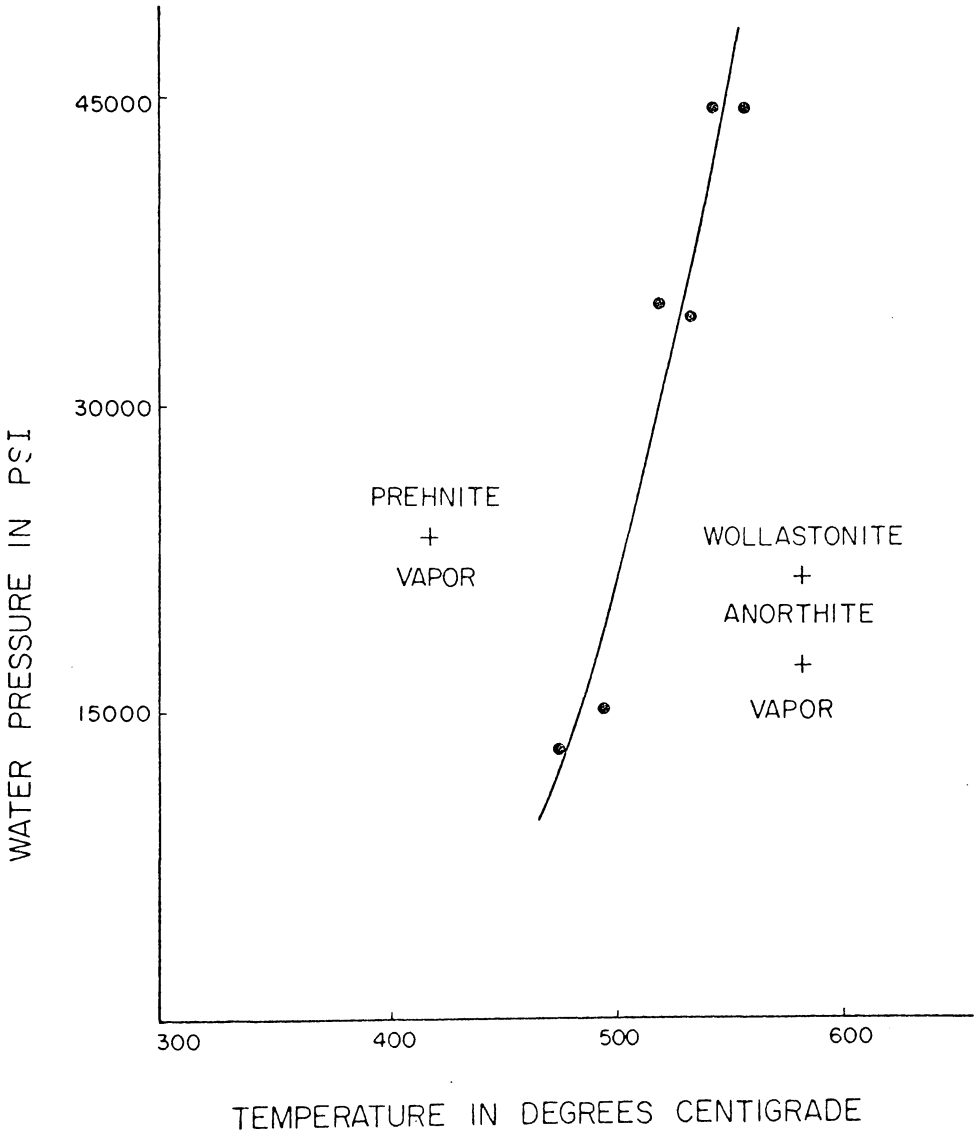

Figure 11. Prehnite Dissociation Curve

The experimental points that limit the placement of the curve are shown as solid dots.

crystal growth occurs. This is directly analogous to the well-known phenomenon that a supercooled liquid will crystallize into many small nuclei. This is partly controlled by the mobility of the ions and complexes upon dissociation. The importance of the mobility factor becomes apparent when water pressure is increased. Fewer nuclei are formed at higher water pressure and therefore larger crystals result. This greater mobility at higher water pressure may be due to the increased solubility of the ions and complexes in the water.

The three-phase triangle wollastonite-anorthite-grossularite shown in Figure 12 illustrates how compositional variations can change the equilibrium assemblages. At temperatures below the dissociation of prehnite addition of $CaO-SiO_2$ to anorthite would produce a stable assemblage of prehnite and anorthite. This is a realistic situation geologically and is discussed in Chapter 6. Similarly, a $(CaO-SiO_2)$-prehnite assemblage would be stable were $SiO_2-Al_2O_3$ added to wollastonite; however, this has little geologic application.

Grossularite was produced as a decomposition product of prehnite in all experimental runs, including those below the dissociation curve of prehnite (Fig. 11). The assemblages prehnite-grossularite or anorthite-wollastonite-grossularite can be explained by analyzing the stability field outlined on the $CaO-SiO_2-Al_2O_3$ diagram in Figure 12. It can be seen that if the prehnite sample is CaO rich, e.g., Point (B) on Figure 12, grossularite could form at the expense of the CaO-rich prehnite. This would move the composition of the unreacted prehnite towards the theoretical composition of stoichiometric prehnite, Point (Pr) on the diagram. An example of this reaction is as follows:

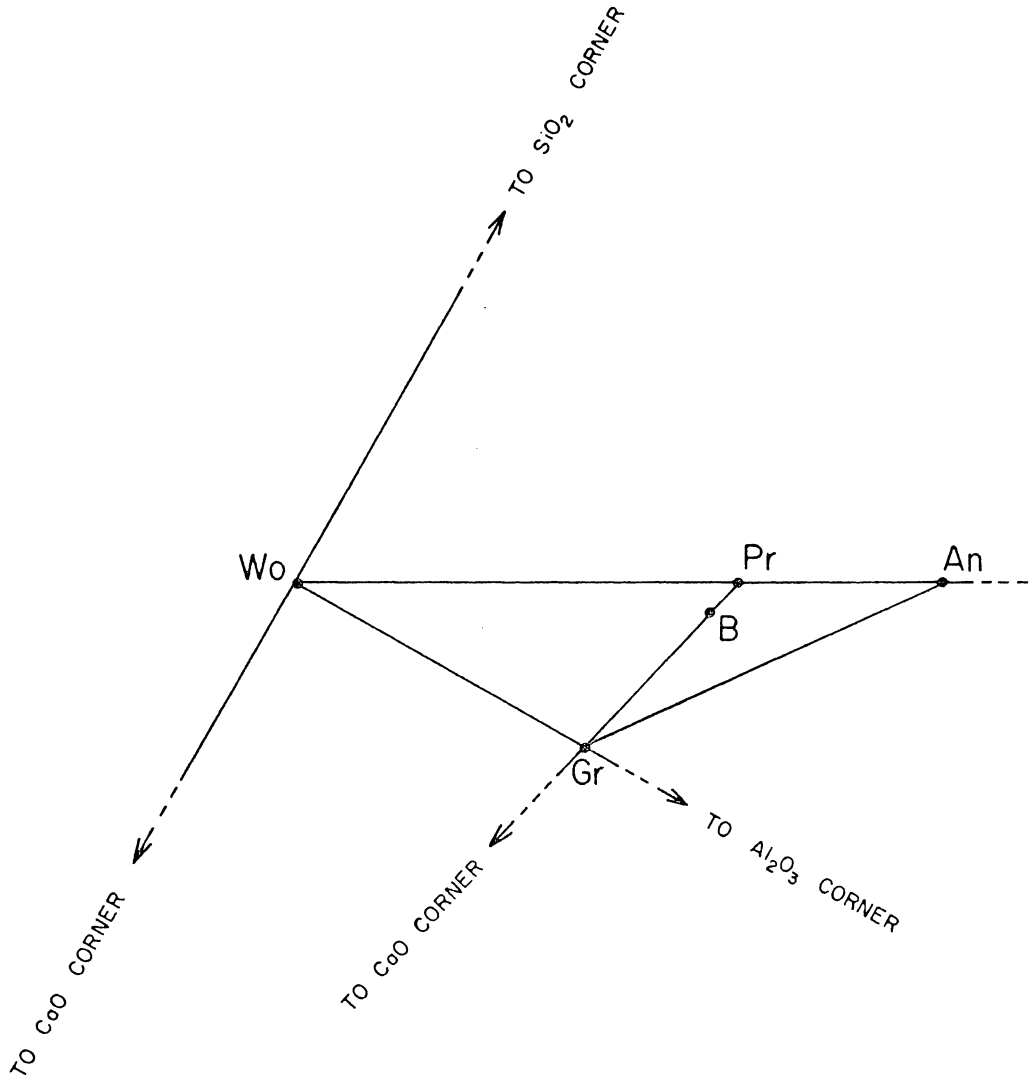

Figure 12. Portion of the System $CaO-SiO_2-Al_2O_3-H_2O$

The anhydrous base of the system $CaO-SiO_2-Al_2O_3-H_2O$ is shown with the composition point of prehnite projected into the $CaO-SiO_2-Al_2O_3$ composition plane. Point B represents an off-composition prehnite.

$$11Ca_{2.09}Al_2Si_3O_{10.18}(OH)_{1.81} \rightleftharpoons 10Ca_2Al_2Si_3O_{10}(OH)_2 + Ca_3Al_2Si_3O_{12}$$

$$\text{CaO-rich Prehnite} \rightleftharpoons \text{Prehnite} + \text{Grossularite}$$

The decomposition of the CaO-rich prehnite at composition (B) to grossularite can occur at a lower temperature and/or higher pressure than the decomposition of prehnite of composition (Pr) in Figure 12. This interpretation is based on the fact that grossularite formed in all experimental runs, when given sufficient time. The nonstoichiometry of the original prehnite sample did not appear to have an effect on the dissociation curve of prehnite. The dissociation curve was therefore based on the appearance of wollastonite and anorthite rather than on the appearance of grossularite.

No recrystallization producing secondary prehnite was noted; therefore, it was concluded that the calcium was removed from the Ca-rich prehnite without destroying its structure. This removal of calcium may be an exsolution phenomenon, in which case it could exsolve at various temperatures rather than at one definite temperature. If this were the case, prehnites with different amounts of calcium may dissociate at different temperatures depending upon the initial amount of calcaium. Another possibility is that a small amount of calcium is held interatomically. In this respect the prehnite would be similar to the zeolites with which it is often associated. This reaction could be simply written as

$$CaO + Ca_2Al_2Si_3O_{10}(OH)_2 \rightleftharpoons Ca_3Al_2Si_3O_{12}.$$

In this reaction, it is unlikely that the formation of the grossularite would alter the dissociation temperature of prehnite.

Figure 13 illustrates the mechanism by which the assemblage grossularite-anorthite-wollastonite is formed. Calcium-rich prehnite decomposes to form an assemblage of grossularite and prehnite at some temperature (T_1). With further heating the prehnite decomposes to form wollastonite and anorthite (475°C and 1000 bars water pressure). This is summarized by the following equations:

$$CaO + 11Ca_2Al_2Si_3O_{10}(OH)_2 \rightleftharpoons 10Ca_2Al_2Si_3O_{10}(OH)_2 + Ca_3Al_2Si_3O_{12}$$

$$10Ca_2Al_2Si_3O_{10}(OH)_2 \rightleftharpoons 10CaAl_2Si_2O_8 + 10CaSiO_3 + 10H_2O.$$

Adding the two above equations together gives:

$$CaO + 11Ca_2Al_2Si_3O_{10}(OH)_2 \rightleftharpoons 10CaAl_2Si_2O_8 + 10CaSiO_3 + Ca_3Al_2Si_3O_{12} + 10H_2O.$$

This final equation represents the reaction which takes place at temperatures and pressures above the stability of prehnite. The occurrence of grossularite will be discussed in greater detail in Chapter 5.

Thermodynamic Considerations and Extrapolations

The prehnite dissociation curve is well documented experimentally above 12,000 psi water pressure in this paper. However, because of the slow reaction rates at low water pressures, no reliable data were obtained below this pressure. For example, at 7500 psi water pressure the reaction does proceed, but only at elevated temperatures, producing a curve that is inconsistent with the data for the samples subjected to pressures of 12,000 psi or more.

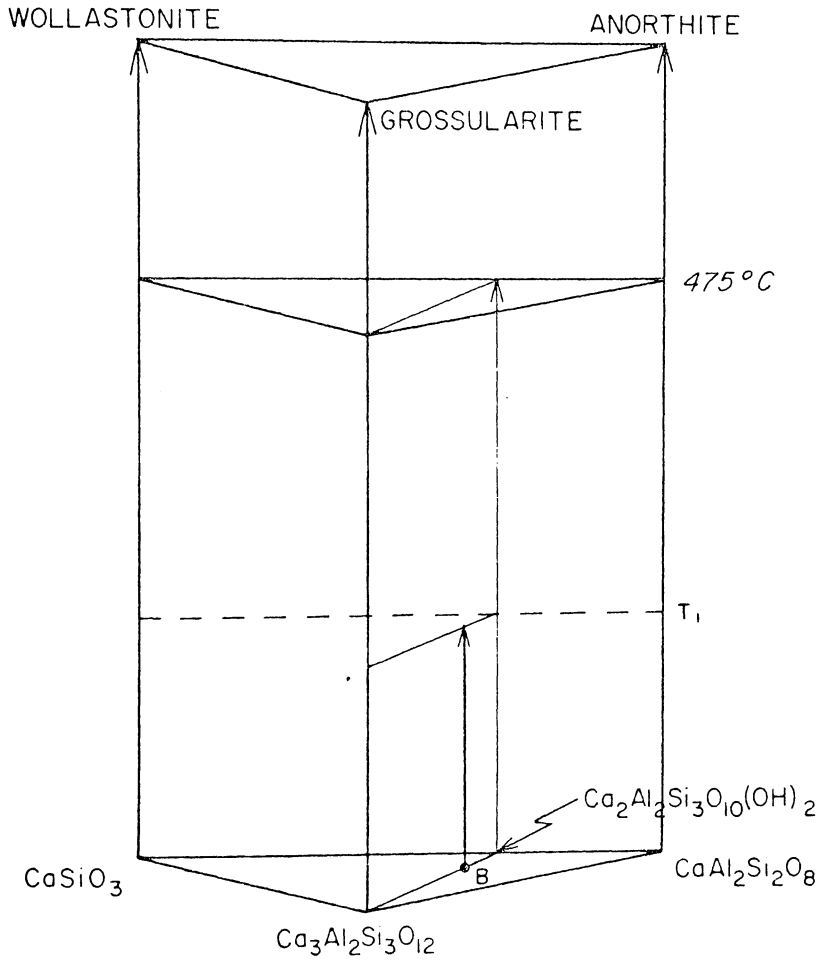

Figure 13. Mechanism for Grossularite-Wollastonite-Anorthite Coexistence

The coexistence of wollastonite-anorthite-grossularite can be explained using the following mechanism, based on a CaO-rich prehnite, Point B on the diagram.

CaO-rich Prehnite ⇌ Grossularite + Prehnite
Prehnite ⇌ Anorthite + Wollastonite

CaO-rich Prehnite Anorthite + Wollastonite + Grossularite

It is therefore necessary to extrapolate the experimental results to lower temperatures and pressures in order to encompass the near-surface conditions under which prehnite forms as open-space cavity fillings. To accomplish this, a thermodynamic approach based on the Clapeyron equation has been used.

$$\frac{dP}{dT} = \frac{\Delta H}{T \Delta V}.$$

This equation gives the slope (dP/dT) of the phase boundary at the point where the temperature is equal to (T). ΔH is the change in enthalpy (heat of reaction) across the phase boundary at that point and ΔV is the change in volume. Using this equation over small increments of the curve in which the slope can be considered constant, the change in the enthalpy for the reaction can be calculated. Integration of the above equation gives the following form:

$$P_2 - P_1 = \frac{\Delta H}{\Delta V} \ln (T_2/T_1).$$

This equation can be used to project a true curved extrapolation of a phase boundary rather than a straight line projection, as is given by the Clapeyron equation. The success of the integrated form is dependent upon ΔH and ΔV, for it is essential that both remain reasonably constant along the phase boundary. Therefore, evaluation of theΔH and ΔV along the experimentally determined portion of the phase boundary gives some insight into the usefulness of the integrated form of the Clapeyron equation.

A graph showing the rate of change of ΔV along the experimentally determined portion of the prehnite dissociation curve is shown in Figure 14. The change in volume across the curve (ΔV) is calculated in the following manner. The molar volumes for the solid phases encountered are considered constant at all temperatures and pressures and are given by the Chemical Rubber Company Handbook (1968) as follows:

Prehnite	141.73 cc/mole
Anorthite	100.93 cc/mole
Wollastonite	39.94 cc/mole.

The molar volume of the water evolved from the dissociation of prehnite is dependent upon the temperature and pressure and therefore cannot be considered constant. The molar volume of water at various temperatures and pressures is obtained from Kennedy and Holser's (1966) data on the specific volume of water. The molar volume of the products minus the molar volume of the reactants at any given temperature and pressure on the phase boundary gives the ΔV for the reaction at that point. These values are plotted on Figure 14. It can be seen from this graph that the ΔV for the reaction is not constant but does define a smooth curve.

The calculations of the enthalpy of reaction (ΔH) at various points along the experimentally determined dissociation curve (Fig. 11) can be made through the use of the Clapeyron equation. In making these calculations, pressure intervals of 500 bars water pressure were used with the corresponding temperatures to establish the slope of a small increment. ΔH was then calculated using the temperature and change in volume of the reaction (ΔV) at both ends of the 500 bar water pressure

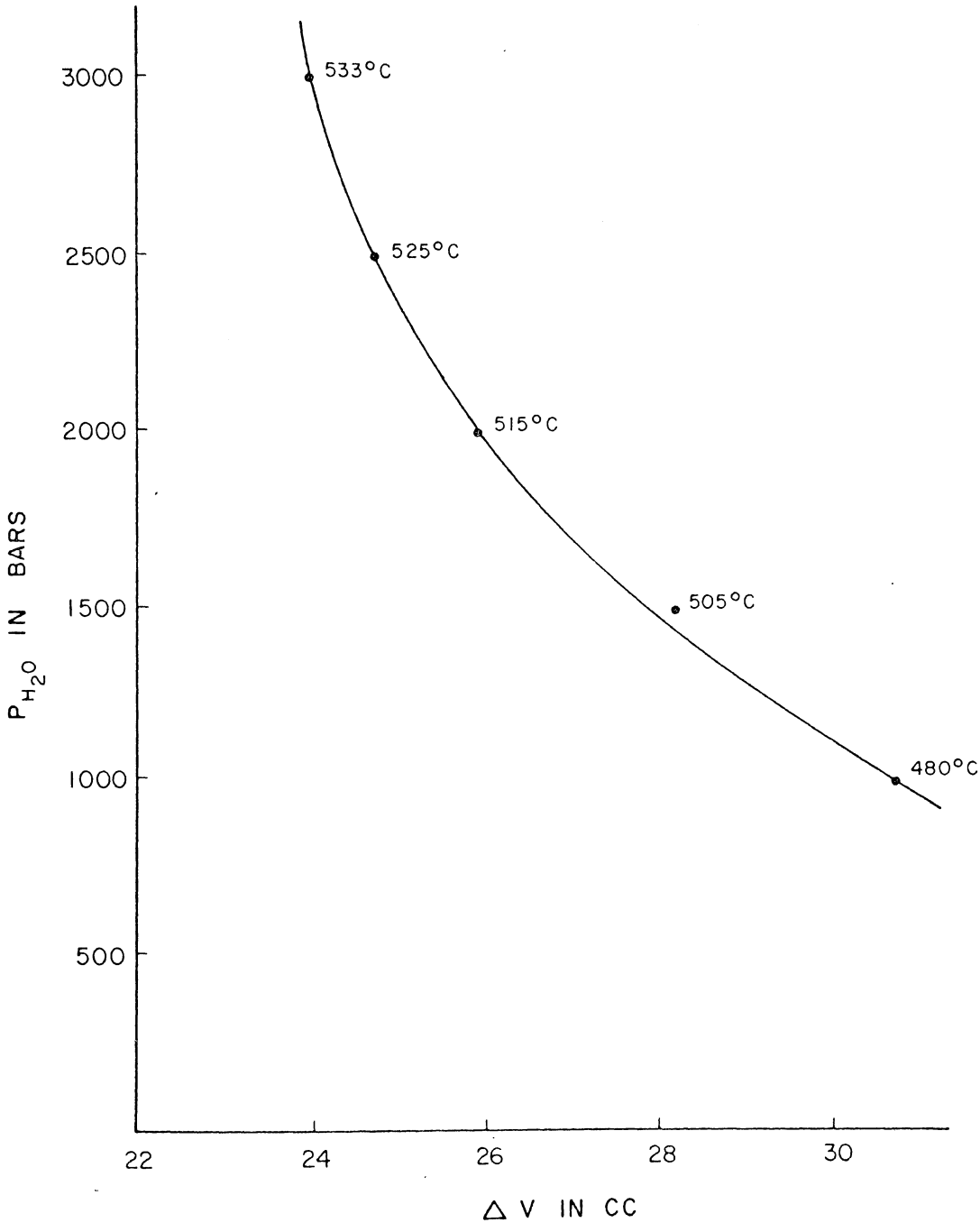

Figure 14. Change in Volume vs. Pressure

increment, giving upper and lower values for the temperature intervals. These values for the enthalpy of reaction (ΔH) were then plotted and averaged in Figure 15. The data used to calculate the points depicted in Figure 15 are shown in Table 3.

The points depicting the average values of the enthalpy of reaction (ΔH) are the result of two independent calculations. The points designated (A) were determined by averaging the two limits of the 500 bar water pressure increment. The points designated (B) were determined by averaging the two enthalpies of reaction at a given isobar. These averages are a reasonable estimate of the actual value; however, the enthalpy may vary anywhere between the two extreme values shown in Figure 15. For example, at 15,000 psi the maximum error in the enthalpy is $\pm$ 22%. However, there is reason to believe that the average values calculated have a much smaller error factor.

Taking the two factors, ΔV and ΔH, into consideration, then it is apparent that the integrated form of the Clapeyron equation cannot be used. Neither ΔV nor ΔH remain constant along the phase boundary as is required for the required for the relationship to be valid.

A more meaningful extrapolation is a semi-quantitative approach to these data, using the phase diagram for water as a reference. Assuming that the molar volumes of the solid phases do not change significantly, it can be stated that the change in the ΔV of the reaction is a function of the change in volume of water. In Figure 16 the experimentally determined dissocation curve for prehnite is superimposed on the diagram of the specific volume of water (Kennedy, 1950a). It can be seen that the that the specific volume of water increases with decreasing pressures

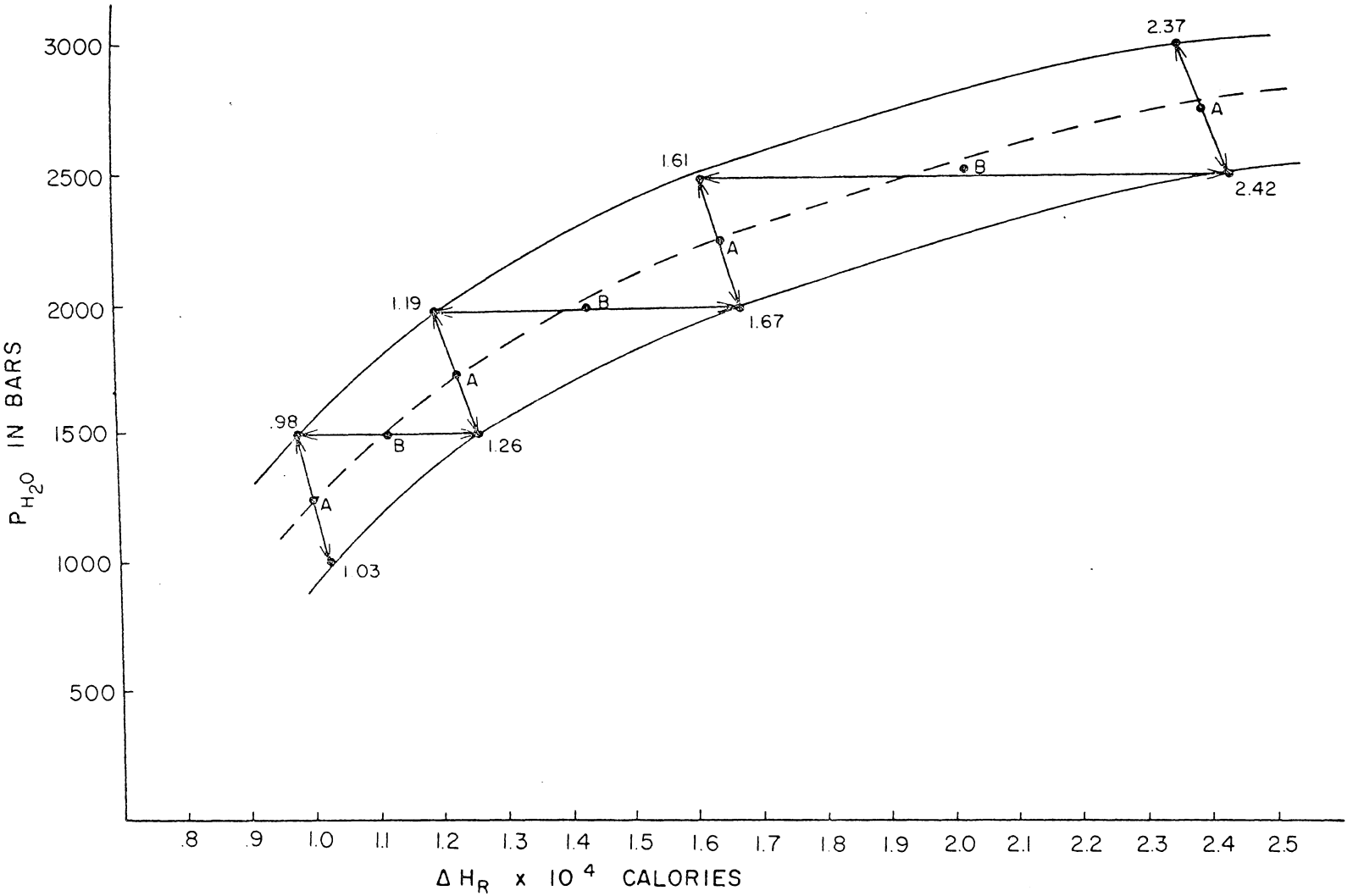

Figure 15. Plot of Enthalpy of Reaction vs. Pressure

TABLE 3

ENTHALPY DATA

WATER PRESSURE	TEMP.°K	Δ V	Hi VALUE OF Δ H IN CALORIES	Lo VALUE OF Δ H IN CALORIES
1000 bars	748	30.62	1.03×10^4	
1500 bars	775	28.23	1.26×10^4	6.98×10^4
2000 bars	796	25.83	1.67×10^4	1.19×10^4
2500 bars	811	24.65	2.42×10^4	1.61×10^4
3000 bars	821	23.90		2.37×10^4

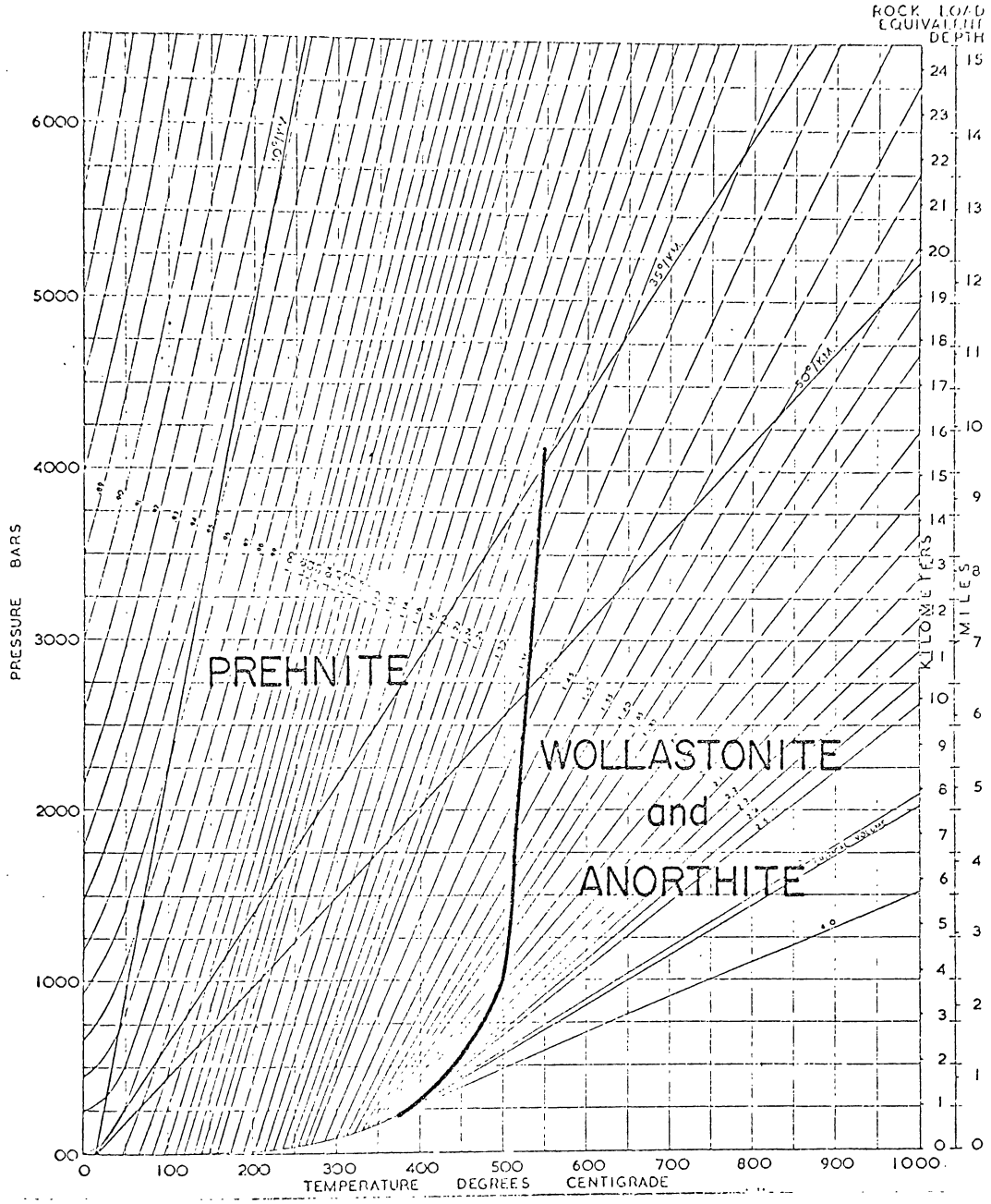

Figure 16. P-T-V Relations of Water with the Prehnite Dissociation Curve Superimposed

along the curve. This produces the change in ΔV of the reaction as shown in Figure 14.

If at low water pressure the dissociation curve trends along line A—B in Figure 17, the ΔV for the reaction would begin to decrease. To maintain the slope from A to B and remain within the liquid portion of the water phase diagram, ΔH for the reaction would have to decrease to about 84 calories per mole. As the trend of the enthalpy of reaction (Fig. 15) differs widely from this, it is an unlikely solution to the problem. If the curve is extrapolated below the critical point of water, the ΔV for the reaction becomes very large, i.e., doubled or tripled. This large increase in ΔV forces the curve to become tangential to the water-liquid, water-vapor phase boundary at low water pressures. Line A—C on Figure 17 shows this relationship. This also satisfies the trend of ΔH as shown in Figure 15.

Figure 18 shows the relationship between the extrapolated curve and the two factors controlling its slope, ΔH and ΔV. This compilation of the data points out the validity of this approach.

A pattern of this type is possible for the dissociation curve for other hydrated minerals. With decreasing pressure, the temperature of dissociation also decreases. This has been verified at elevated temperatures and pressures by those who have determined these curves; However, experimental techniques have not allowed significant data to be obtained at low water pressures. It appears that at low water pressure the dissociation temperatures for other hydrated minerals would also decrease considerably. Mineral assemblages which are normally considered to be stable at high temperatures may also be stable at

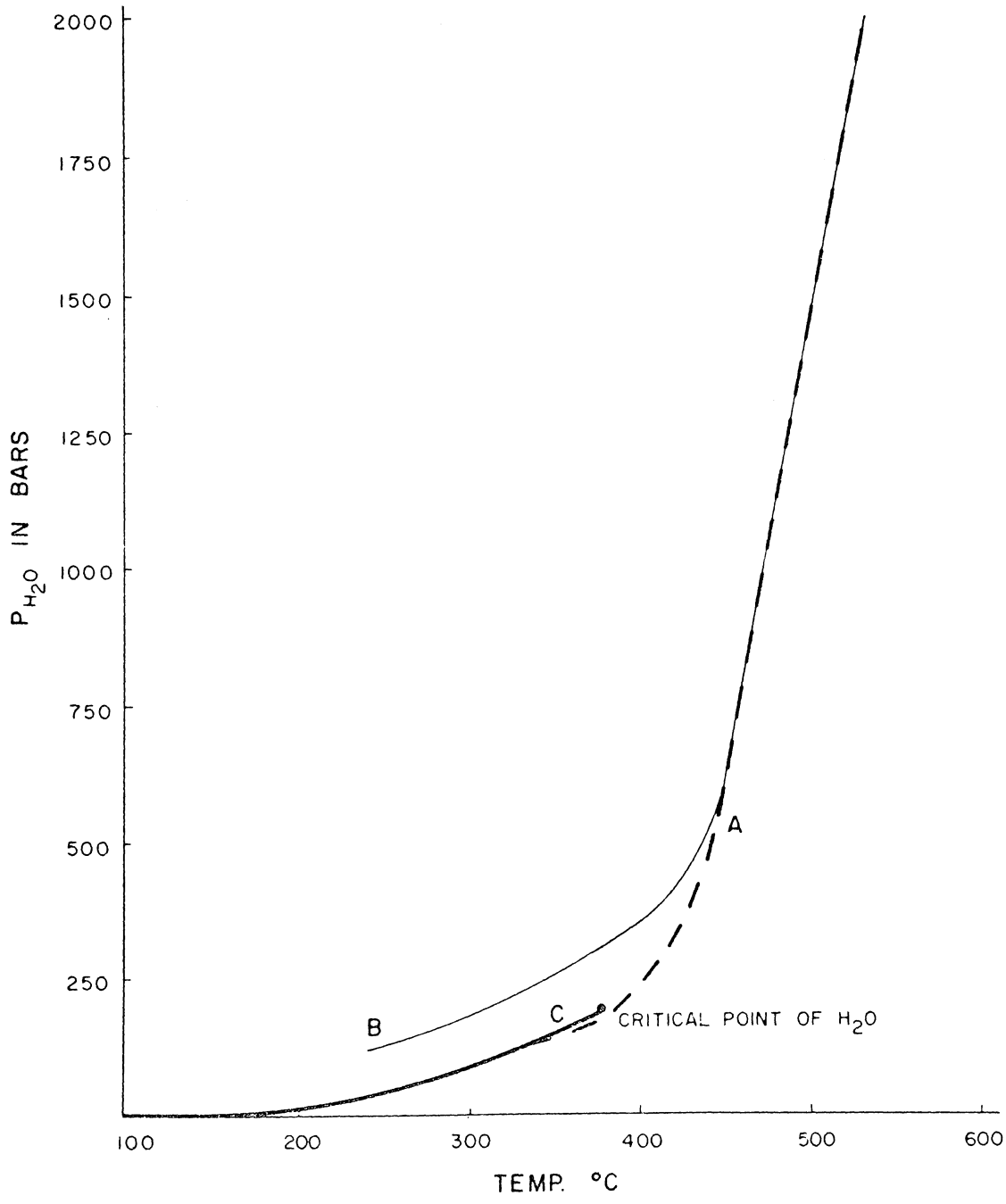

Figure 17. Extrapolation of the Prehnite Dissociation Curve to Low Temperatures and Pressures

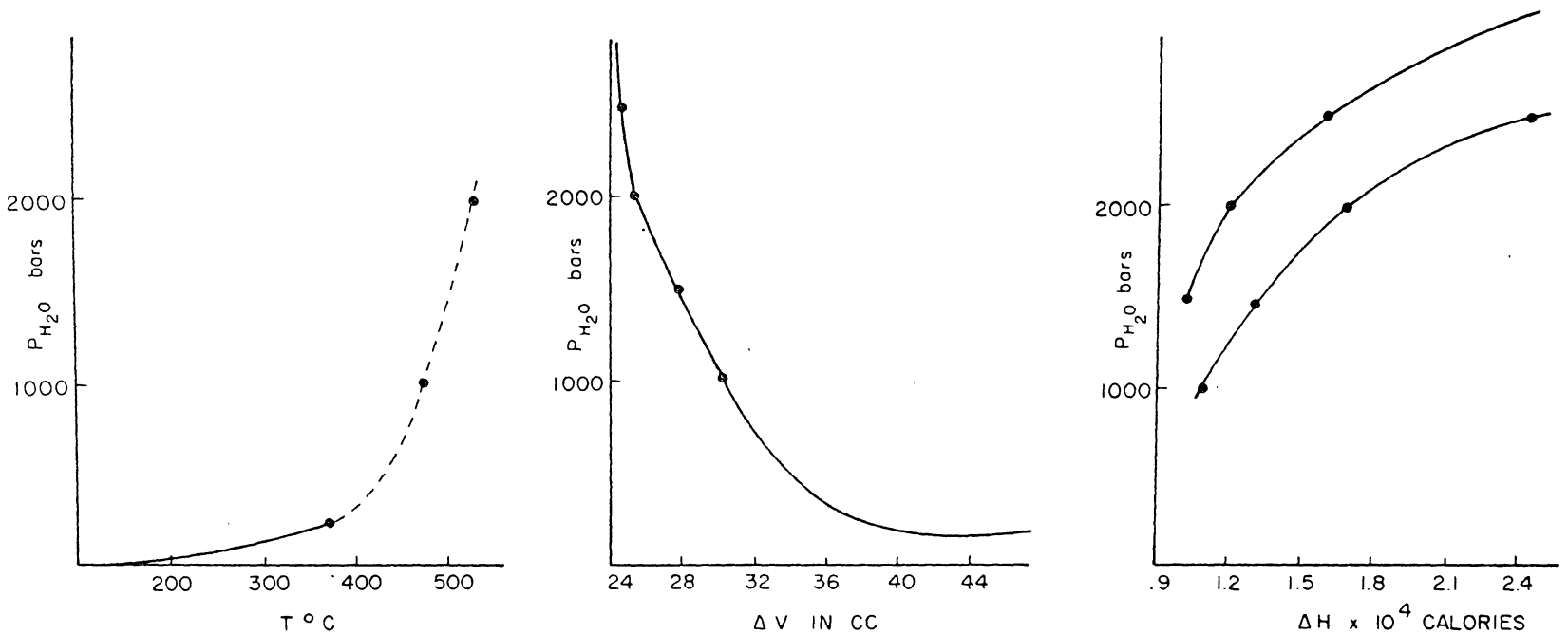

Figure 18. Diagrams Relating ΔV and ΔH for the Reaction $Ca_2Al_2Si_3O_{10}(OH)_2 \rightleftharpoons CaSiO_3 + CaAl_2Si_2O_8$ to the Dissociation Curve of the Same Reaction

reasonably low temperatures, e.g., wollastonite, anorthite, and water could be stable below 300°C. An interesting area for further research would involve the extrapolation of dissociation curves for hydrated minerals to low water pressures and their relationship to the water phase diagram.

CHAPTER V

THE GROSSULARITE PROBLEM

It has been pointed out in earlier chapters that grossularite is ubiquitous in the experimental runs. In optical oil mounts it comprises approximately 10 percent in the plan view, apparently a significant amount. Its presence has posed a question concerning the composition of the prehnite-water system and the mechanism producing the grossularite. The enlarged portion of the CaO-SiO_2-Al_2O_3 diagram (Fig. 12) suggests that the system is calcium rich. This is a necessary conclusion based on the coexistence of wollastonite, anorthite, and grossularite.

A short review of the decomposition sequence discussed in Chapter 4 (Experimental Results) can be made by following the steps through Figure 13. Ca-rich prehnite, Point B, decomposes to form an assemblage of grossularite and prehnite at some temperature (T_1). With further heating, prehnite decomposes to form wollastonite and anorthite. These two reactions produce a stable assemblage of wollastonite, anorthite, and grossularite.

Several mechanisms have been examined in order to determine the source of the apparent calcium enrichment. One possible mechanism is that SiO_2 is sufficently soluble in the water at the prescribed temperatures and pressures to essentially enrich the solids of the system in CaO and Al_2O_3. A second possibility is improper sample preparation

resulting in contamination with calcite, $CaCO_3$. This is possible because the prehnite is intimately intergrown with calcite in the hand specimen. However, extreme care was taken to protect against such contamination. A third possibility is that the natural prehnite is non-stoichiometric. This could result from minor solid solution within the prehnite structure, enriching it in calcium. Small amounts of calcium could also be held interatomically with prehnite behaving in a manner similar to the zeolites. It should be noted that either enrichment in calcium or deficiencies in SiO_2 and Al_2O_3 produce the same results. Through the course of this investigation all three of the above mechanisms were considered likely, and only through experimentation and calculations was the most probable solution determined.

SiO_2 Solubility

The possibility of silica solubility in the water included with the sample is a satisfying idea. This mechanism of grossularite formation would have little effect on the stability of prehnite, the determination of which is the main purpose of the investigation. To resolve this problem experimental runs with no water, 10 percent by weight water, and 50 percent by weight water were made, runs P-14, P-15, and P-16, respectively. If silica solubility were important, then considerably more grossularite would form in the run with 50 percent by weight water than in the other two runs, P-14 and P-15. It was found that all three runs produced similar amounts of grossularite, approximately 10 percent in plan view. Strong evidence proving silica solubility to be unimportant in the formation of grossularite is given by the following calculations

which uses data on silica solubility in water (Kennedy, 1950b) At 475°C and 1000 bars water pressure there is 0.228 weight percent SiO_2 in silica saturated water. This is equivalent to

$$(0.228 \text{ wt.\%})\ (18.04 \text{ gm of solution}) = 0.041 \text{ gm}$$

of SiO_2 in one mole of H_2O. The reaction

$$Ca_2Al_2Si_3O_{10}(OH)_2 \rightleftharpoons CaAl_2Si_2O_8 + CaSiO_3 + Ca_3Al_2Si_2O_{12} + H_2O$$

occurred experimentally in 20% by weight water. When considering one mole of reactants (412 gm), 20% by weight water would be equivalent to

$$(412 \text{ gm})\ (.20) = 82.4 \text{ gm}$$

or 4.59 moles of H_2O and therefore

$$(4.59 \text{ mole } H_2O)\ (0.04 \text{ gm } SiO_2/\text{mole } H_2O) = 0.17 \text{ gm } SiO_2$$

in the total amount of water in the run, i.e., 16.66 weight percent. From the reaction

$$3Ca_2Al_2Si_3O_{10}(OH)_2 \rightleftharpoons 2Ca_3Al_2Si_3O_{12} + 3SiO_2 + Al_2O_3 + H_2O$$

the ratio of moles of grossularite to moles of SiO_2 is 2 to 3. The number of moles SiO_2 can be calculated as follows:

$$(0.17 \text{ gm } SiO_2)/(60 \text{ mg/mole } SiO_2) = .0028 \text{ mole } SiO_2$$

dissolved in water. Using the ratio of 2 to 3 it can be shown that

0.0018 mole of grossularite are produced due to silica solubility. This computes to 0.87 gm grossularite or .21 weight percent.

It can easily be seen from the calculations that silica solubility in water cannot be responsible for the formation of the grossularite. An interesting note, however, is that in runs which failed due to capsule leakage, up to 25–30 percent grossularite was formed. It is believed that silica solubility becomes important when the sample is exposed to the overwhelming amount of water held in the pressure system.

Calcite Contamination

The possibility of improper sample preparation was also considered. The prepared sample powder was immersed in hydrochloric acid and observed closely for any effervescence; none was observed. The material was then leached in hydrochloric acid and used in an experimental run (sample P-41). An unleached sample (P-42) was run simultaneously with the leached sample for comparison. Optical analysis showed that the leached material had produced less grossularite, though not significantly less. The reduction in grossularite could be a direct result of leaching of some calcite; however, the fact that grossularite persists in significant amounts indicates that this is not the primary mechanism. Deer et al. (1962) state that prehnite is slightly soluble in hydrochloric acid and forms a gelatinous material upon prolonged leaching. It is possible that the leaching partially dissolved the prehnite and removed some of the calcium from its structure to produce a less CaO-rich prehnite. If this were true, there need not be any calcite present in the sample for grossularite to form. This indirect evidence suggests that

the presence of calcite is not responsible for the formation of the grossularite.

The possibility of calcite contamination points out further possible studies. Naturally occurring prehnite is often associated with calcite, formed under temperature and pressure conditions where both minerals were stable. Experimental runs P-9 and P-40 show that prehnite and calcite are an unstable assemblage at elevated temperatures and water pressure and combine to form grossularite at low CO_2 pressures. The following equation illustrates this point:

$$Ca_2Al_2Si_3O_{10}(OH)_2 + CaCO_3 \rightleftharpoons Ca_3Al_2Si_3O_{12} + H_2O + CO_2.$$

Because grossularite is present in all runs and forms from a Ca-rich prehnite, it is suggested that the above reaction takes place at temperatures lower than the prehnite dissociation curve (Fig. 11). This curve would be dependent upon temperature, H_2O pressure and CO_2 pressure. In addition, an interesting reaction would occur in a prehnite-calcite-water system. Here, the beginning of reaction would be essentially at zero CO_2 pressure; this would also be the minimum temperature at which grossularite, H_2O, and CO_2 could coexist at equilibrium. An increase in CO_2 pressure would drive the reaction toward the prehnite-calcite assemblage and therefore raise the reaction temperature. Studies of this sort may give some insight into the conditions prevailing when prehnite is formed in nature. It could also be interesting with respect to grossularite, since it would determine the minimum temperature at which grossularite could coexist with H_2O and CO_2 in rocks such as skarns.

Non-stoichiometric Prehnite

Solid solution within the prehnite structure was considered early as a possible solution to the grossularite problem; however, the other mechanisms required testing before being discarded. Solid solution proves to be the most logical and the most convincing hypothesis considered in light of the data.

In comparing the composition from various localities, Table 1, it can be seen that the analyses (Nuffield, 1943) indicate a rather constant composition. It can also be seen that there is a slight but persistent deficiency in silicon with a corresponding excess in aluminum.

Nuffield (1943) structurally analyzed a prehnite from Ashcroft, British Columbia, and deduced the following chemical formula:

$$Ca_{4.06}Al_{3.83}(Si, Al)_{6.00}O_{19.55}(OH)_{4.04}.$$

Assuming that the anorthite, wollastonite, and grossularite have chemical formulae represented by the pure minerals, the following reaction may be written:

$$Ca_{4.06}Al_{3.83}(Si, Al)_{6.00}O_{19.55}(OH)_{4.04} \rightleftharpoons 1.88\ CaAl_2Si_2O_8 + 1.97\ CaSiO_3 + 0.07\ Ca_3Al_2Si_3O_{12} + 2.02\ H_2O.$$

The elements balance as follows:

Reactants		Products			
Ca	4.06	Ca	4.06		
Al	3.83	Al	3.95	Al	3.84
Si,Al	6.00	Si	5.94	Si,Al	6.00
O	23.59	O	23.81		
H	4.04	H	4.04		

It can be seen by comparing the number of moles of each element in the products to the number of moles in the reactants that the equation is balanced except for minor oxidation. By multiplying the molar volume of each mineral in the reaction by the number of moles of each, respectively, the volume of that many moles can be calculated. The following calculations show this for the products:

Volume Anorthite	(100.75 cc/mole)(1.88)	= 191.29 cc
Volume Wollastonite	(39.37 cc/mole)(1.97)	= 79.52 cc
Volume Grossularite	(125.10 cc/mole)(0.07)	= 8.75 cc
	Total volume of the products	= 279.56 cc

Dividing the volume of grossularite by the total volume gives 3.13 percent grossularite by volume.

To convert the volume data to area in plan view, as is seen through the petrographic microscope, it is necessary to make a few assumptions. The first assumption is that the wollastonite and anorthite grains are four times larger in diameter than the grossularite grains. Optical studies of all-important experimental runs show this to be a good approximation. Using the equation of the volume of a sphere, $V = 4/3\pi r^2$, each anorthite or wollanstonite grain has 64 times the volume of a single grossularite grain. Remembering that the reaction produces 3.13 percent grossularite by volume, the following equation is used to calculate the number of grossularite grains per anorthite or wollastonite grain.

$$(0.0313)(64 + X) = X,$$

where X equals the number of grossularite grains per anorthite or wollastonite grain. As X = 2.064, the reaction produces 2.064 grossularite grains 1/4 the diameter of an anorthite or wollastonite grain per anorthite or wollastonite grain. Using the equation for the area of a circle, $0.7854d^2$, the percent grossularite in plan view can be computed.

2.064 Gross. grains	(d = 1) gives	2.064(0.7854)	units of area
1.000 An or Wo grain	(d = 4) gives	16 (0.7854)	units of area
	total gives	18.064(0.7854)	units of area

Dividing the total area into the area of 2.064 grossularite grains computes to 11.42 percent grossularite in plan view. This value closely agrees with the estimated 10 percent in plan view seen in the oil mounted products.

Having considered three possibilities for the origin of the grossularite, it seems most likely that non-stoichiometric prehnite best explains the occurrence of grossularite. To help resolve the problem, a chemical analysis was done by Schwarzkopf Microanalytical Laboratory. The first analysis done showed a residual of 22 percent, when considering the following oxides: CaO, Al_2O_3, SiO_2, Na_2O, Fe_2O_3, FeO, CO_2, and H_2O. It seemed unrealistic that there could have been 22 percent residual, so a duplicate analysis was requested. This second analysis totaled to 100.3 percent and is listed in Table 4. Although the weight percent of all oxides total to approximately 100 percent, the author still questions the validity of the analysis.

Figure 19 shows the relationship between the Schwarzkopf analysis (Point B) and analyses taken from Nuffield (1943). All prehnites,

TABLE 4

CHEMICAL ANALYSIS REPORTED BY SCHWARZKOPF MICROANALYTICAL LABORATORY, WOODSIDE, NEW YORK

CaO	26.8
Al_2O_3	19.9
SiO_2	45.2
Na_2O	0.7
K_2O	1.1
Total Fe	1.7
Fe''	0.2
H_2O	4.6
CO_2	0.3
F	0.0
Total	100.3

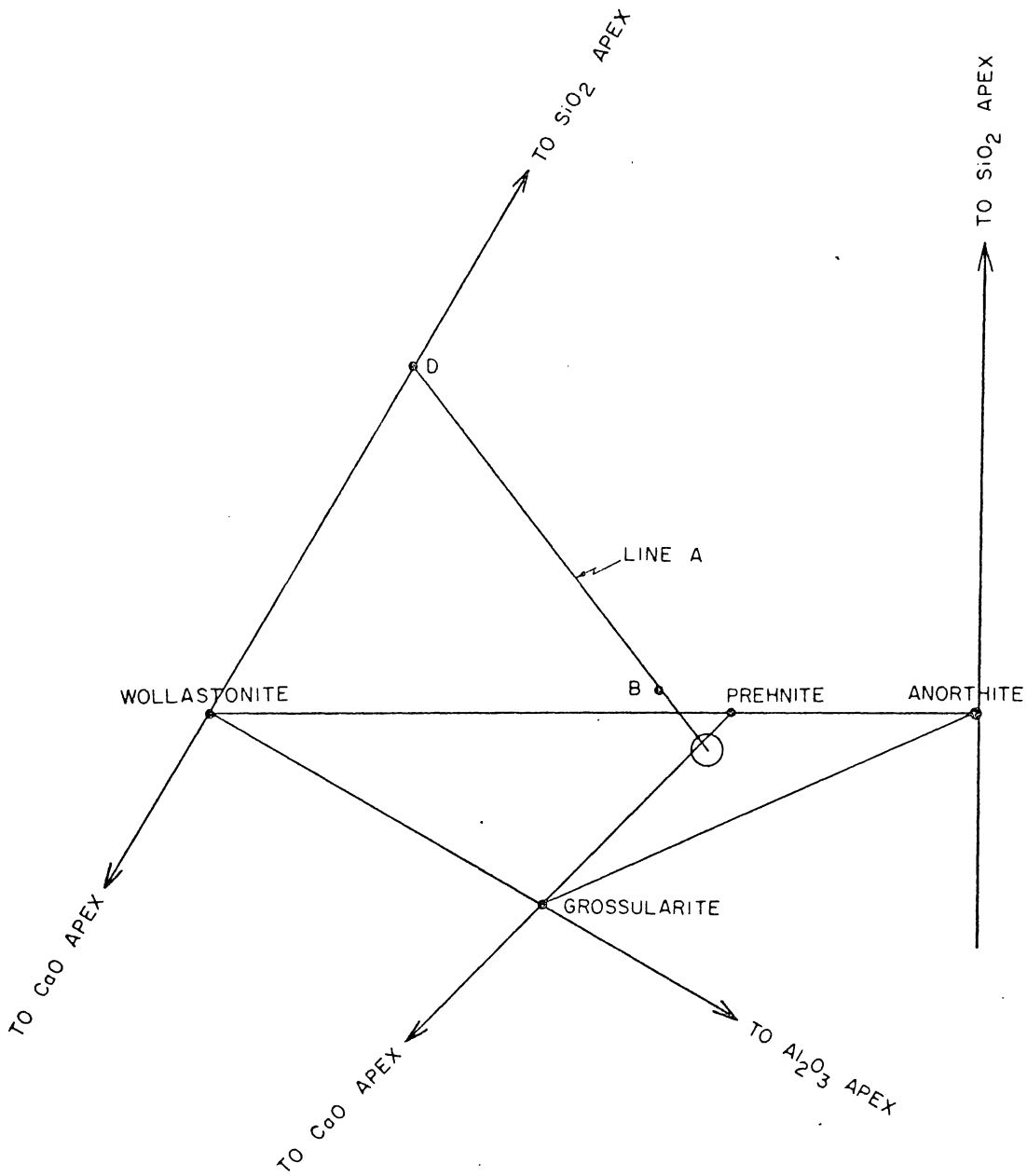

Figure 19. Comparison of Schwarzkopf Chemical Analysis to Prehnite Analyses Cited by Nuffield, 1943

except one, fall within the small circle in Figure 19. The experimental data produced during this investigation indicate that the Patterson, New Jersey, prehnite should have a composition similar to those within the circle. The early formation of grossularite at temperatures below the dissociation curve for prehnite indicates that the original material must have a total composition lying between prehnite and grossularite, as do the prehnites Nuffield cited. The Schwarzkopf analysis of the Patterson, New Jersey, prehnite does not in any way account for the formation of the grossularite, which is well documented experimentally.

Assuming that the Patterson, New Jersey, prehnite is similar to the prehnites Nuffield cited, it would therefore require the presence of another phase or phases to produce the analysis given by Schwatzkopf. Specifically, the bulk composition of this phase or phases would have to lie along line A in Figure 19. If a typical prehnite composition is subtracted from the Schwarzkopf analysis, the bulk composition remaining would fall on the $CaO-SiO_2$ edge of the $CaO-SiO_2-Al_2O_3$ diagram or Point D in Figure 19. Point D has a composition of 61.0 mole percent SiO_2 and 39.0 mole percent CaO ($CaCO_3$). The tie lines between Point D and the circle show that 13.7 mole percent of the composition of Point D is required. A phase of the composition exhibited at Point D is unreasonable. However, quartz and calcite are likely contaminants. It would require 8.4 mole percent quartz and 5.3 mole percent calcite. Considering the care used during the sample preparation, it is unlikely that contaminants such as these would have been unnoticed. It is therefore concluded that the experimental data are correct and invalidate the chemical analysis of the Schwarzkopf Microanalytical Laboratory. For the

purpose of this investigation, it is therefore necessary to exclude the chemical analysis as evidence.

A gel of stoichiometric prehnite composition was prepared to resolve this problem of composition. Experimental runs P-59 and P-61 produced wollastonite and anorthite and no observable grossularite. Reaction rates were such that the wollastonite and anorthite had poor crystal definition. When calcite was added to the prehnite gel (P-62) grossularite formed. In experimental run P-63 quartz was added to the gel; the quartz appeared unaltered, whereas the gel formed poorly crystallized wollastonite and anorthite. It is concluded from these few experimental runs that the Patterson, New Jersey, prehnite is non-stoichiometrically rich in calcium, where the chemical analysis showed otherwise.

CHAPTER 6

PETROLOGIC INTERPRETATIONS

In recent years prehnite has been recognized as an important rock-forming mineral. This recognition has resulted from the discovery that prehnite forms under a wide range of geologic conditions. Notably, it occurs as cavity fillings in basaltic rocks and as an important mineral of low-grade regional metamorphism. Petrologic interpretations, which give considerable insight into the conditions of origin, gain importance in light of this increasing interest.

Correlation to Metasomatic Prehnite

Even though prehnite occurs in a wide variety of geologic environments, several aspects of its formation are constant. Of primary importance is the fact that prehnite is almost always a product of plagioclase alteration; most notable from Ca-rich members of the plagioclase solid solution series. This alteration of Ca-rich plagioclase, or "prehnitization," is in many respects analogous to sausseritization. Prehnitization is the result of $CaO-SiO_2$ metasomatism, whereas sausseritization may be simply CaO metasomatism of Ca-rich plagioclase (anorthite).

Figure 20 shows the anhydrous base of the system $CaO-SiO_2-Al_2O_3-H_2O$ with mineral compositions projected onto the $CaO-SiO_2-Al_2O_3$ composition plane. The effect of sausseritization can be traced by initially considering a system composed of anorthite, Point (An) in Figure

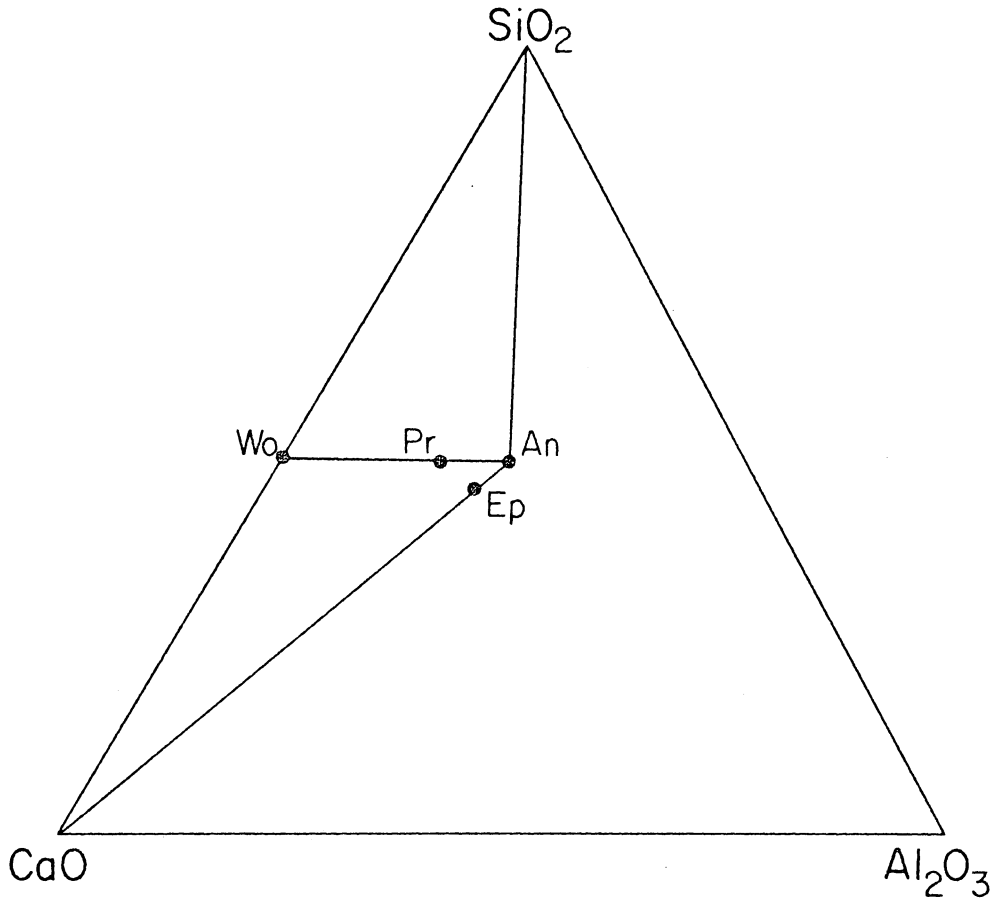

Figure 20. Prehnitization Diagram

The anhydrous base of the $CaO-SiO_2-Al_2O_3-H_2O$ system with prehnite projected onto the $CaO-SiO_2-Al_2O_3$ plane.

20. Under the proper conditions, below the dissociation curve for epidote, CaO metasomatism will change the composition of the system along a line towards the epidote composition (Ep) shown in Figure 20. When the total composition of the system lies between anorthite and epidote, the two minerals can coexist and their relative percentages are given by their tie lines. With further CaO metasomatism the total composition of the system may lie between epidote (Ep) and the CaO apex. Under these conditions the probable mineral assemblage would be calcite and epidote, a common natural association.

Prehnitization is very similar to sausseritization. $CaO\text{-}SiO_2$ metasomatism with equal mole percents of the two species changes the composition of an initially anorthitic system along the line passing through the prehnite composition (Figure 20). When the total composition of the system lies between anorthite and prehnite and the temperature and pressure are such that the prehnite is stable, the two minerals can coexist. This reaction is written as follows:

$$\underset{\text{(anorthite)}}{CaAl_2Si_2O_8} + CaO + SiO_2 + H_2O \rightleftharpoons \underset{\text{(prehnite)}}{Ca_2Al_2Si_3O_{10}(OH)_2}$$

This corresponds with the field occurrence of prehnitized anorthites. If further $CaO\text{-}SiO_2$ metasomatism takes place, the total composition of the system would lie between wollastonite and prehnite. It appears, therefore, that prehnite and wollastonite might be a stable assemblage. However, considering the stability of wollastonite (Fig. 21) and the stability of prehnite (Fig. 11), it is unrealistic to consider a prehnite-wollastonite assemblage in a CO_2-rich environment. Instead, the

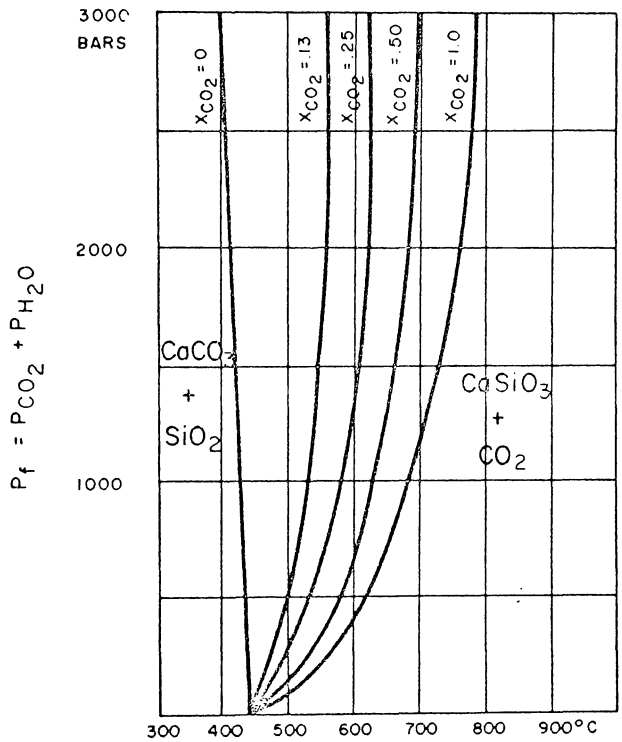

Figure 21. Formation of Wollastonite

Dependence of equilibrium temperatures on the fluid pressure P_f for various constant compositions of the fluid phase (const. X_{CO_2})--Greenwood (1962) and Harker and Tuttle (1956).

assemblage prehnite, calcite, and quartz would exist. The equation showing this assemblage is

$$\underset{\text{(anorthite)}}{CaAl_2Si_2O_8} + 2SiO_2 + 2CaO + H_2O + CO_2 \rightleftharpoons \underset{\text{(prehnite)}}{Ca_2Al_2Si_3O_{10}(OH)_2} + \underset{\text{(calcite)}}{CaCO_3} + \underset{\text{(quartz)}}{SiO_2} .$$

This latter assemblage is very common in low-grade metamorphic environments where CaO-SiO_2 metasomatism has taken place. This may be represented by the three-phase triangle CaO-SiO_2-prehnite (Fig. 22).

Under geologic conditions it would be fortuitous if the metasomatic fluids contained equal mole percents of SiO_2 and CaO. Therefore, it is of interest to consider CaO-SiO_2 metasomatism of greater or lesser amounts of one of the two species. First consider the case in which the mole percent of CaO is less than the mole percent of SiO_2, i.e., $CaO < SiO_2$ metasomatism of anorthite under conditions in which prehnite is stable. If the temperature and pressure conditions are such that heulandite, stilbite, laumontite, or scolecite are unstable, the stable mineral assemblage would be prehnite-quartz-anorthite, which is represented by the three-phase triangle (A) in Figure 23. Under conditions where excess CaO and SiO_2 are present and the anorthite is completely altered to prehnite the stable mineral assemblage is calcite-quartz-prehnite, represented by the three-phase triangle (B) in Figure 23 and by the following equation:

$$\underset{\text{(anorthite)}}{CaAl_2Si_2O_8} + 3SiO_2 + 2CaO + H_2O + CO_2 \rightleftharpoons \underset{\text{(prehnite)}}{Ca_2Al_2Si_3O_{10}(OH)_2} + \underset{\text{(calcite)}}{CaCO_3} + \underset{\text{(quartz)}}{2SiO_2} .$$

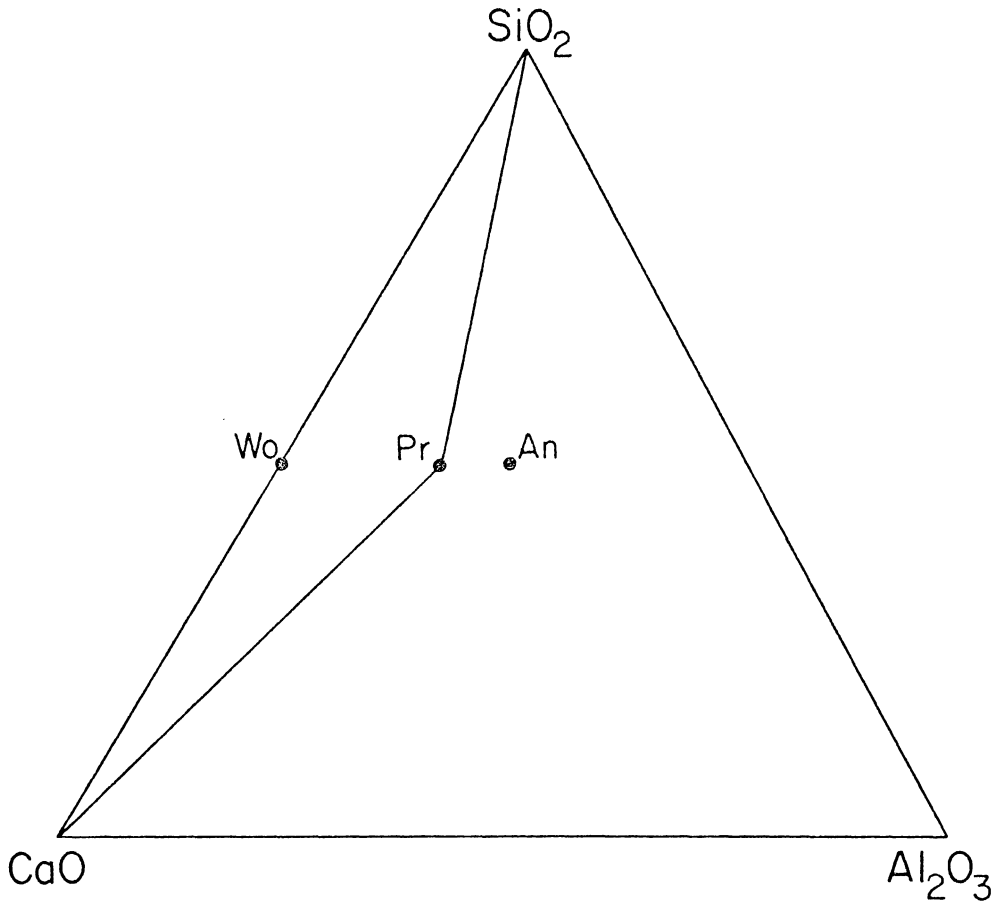

Figure 22. Three-phase Triangle for Low-grade Metamorphism

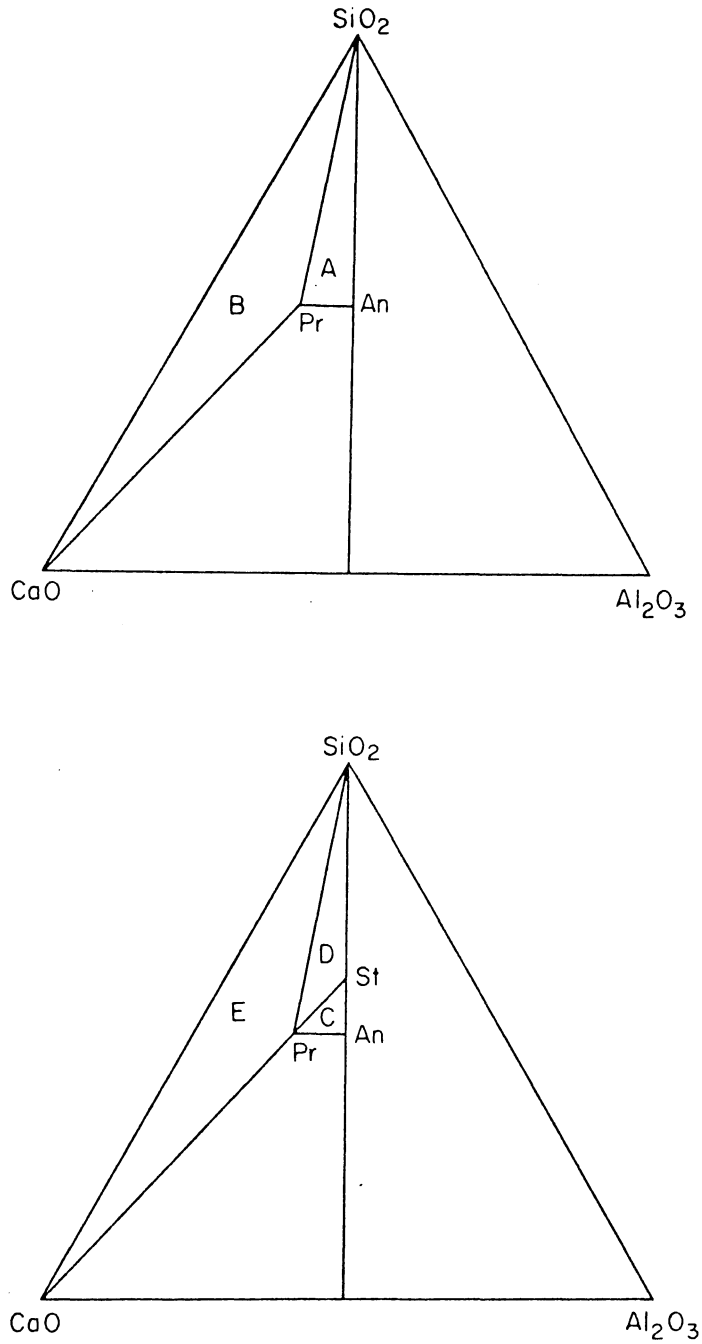

Figure 23. $CaO < SiO_2$ Metasomatism Diagram

If the temperature and pressure conditions are such that heulandite, stilbite, laumontite, or scolecite are stable, the resulting three-phase triangle will depend upon which of these phases is stable. For example, the following equations illustrate $CaO < SiO_2$ metasomatism (Fig 23) with a CaO/SiO_2 ratio of 1/2; with excess CaO considered as calcite; with stilbite the stable mineral rather than anorthite and quartz; and with the reaction stilbite + CaO + prehnite taking place.

Field (C) $3An + 1CaO + 2SiO_2 \rightleftharpoons 1Pr + 1St + 1An$

Field (D) $2An + 2CaO + 4SiO_2 \rightleftharpoons 2Pr + 1St + 1SiO_2$

$3An + 3CaO + 6SiO_2 \rightleftharpoons 3Pr + 3SiO_2$

Field (E) $3An + 4CaO + 8SiO_2 \rightleftharpoons 3Pr + CaCO_3 + 5SiO_2$.

Considering the other alternative, when $CaO > SiO_2$ metasomatism takes place, the following assemblages may coexist and are illustrated in Figure 24.

Field (F) $2An + 2CaO + 1SiO_2 \rightleftharpoons 1Pr + 1An + 1CaCO_3$

$2An + 4CaO + 2SiO_2 \rightleftharpoons 2Pr + 3CaCO_3$

Field (G) $2An + 6CaO + 3SiO_2 \rightleftharpoons 2Pr + 5CaCO_3 + SiO_2$.

The final mineral assemblage stable when anorthite is excluded from the system is the same whether $CaO < SiO_2$ or $CaO > SiO_2$, namely, the mineral assemblage prehnite-calcite-quartz. This assemblage is very common in areas that have undergone extensive "prehnitization."

The dissociation curve for prehnite, Figure 11, defines the upper limit at which a composition similar to the Patterson, New Jersey, prehnite can be stable. The qualification of the material as being from

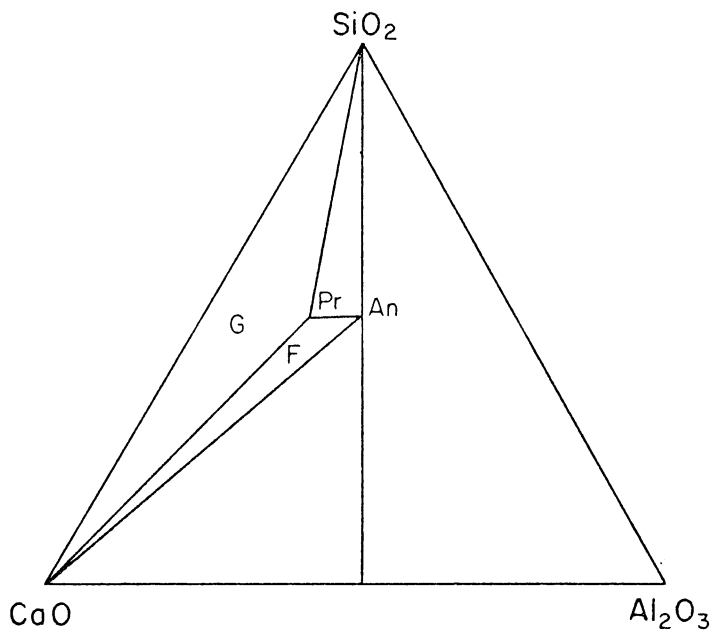

Figure 24. CaO > SiO_2 Metasomatism Diagram

Patterson, New Jersey, is made because the stability of prehnite appears to be very dependent upon composition. This is shown by the fact that prehnite decomposes to form grossularite at a much lower temperature in the presence of calcite, possibly on the order of 100°C lower. Therefore, direct application of the temperatures and pressures defining the dissociation curve for prehnite is difficult. To fully define the conditions under which a particular prehnite assemblage occurs, it will be necessary to work experimentally with the assemblages rather than the individual minerals. Yet, experimental studies of individual minerals, such as this work, must be the beginning point. The obvious sequel to this work is the study of SiO_2-rich prehnite systems and Ca-rich prehnite system, which would more closely approximate the natural occurrence of prehnite.

Prehnite Amygdales in Basalt Flows

There has been considerable controversy as to the time and conditions under which prehnite and zeolite amygdales have formed in extrusive basalts. Being surface phenomena, the pressure at the time of formation should approach one atmosphere water pressure. The author has concluded that in extrapolation of the experimentally determined prehnite dissociation curve to low pressures, the curve becomes tangential to the H_2O (liquid)$-H_2O$ (vapor) phase boundary shown in Figures 16 and 17. It is concluded that other hydrous minerals such as zeolites behave similarly in the low-pressure region. Considering this extrapolation, it can be shown that the formation of the amygdales must have occurred under a temperature and pressure environment of approximately one atmosphere water pressure and less than 100°C.

This conclusion is contrary to the belief that the formation of the amygdales represents the final stages of crystallization of the basaltic flow, i.e., 1000°C. Therefore, the formation of the amygdales had to have occurred at some time later when the flow had cooled to less than 100°C. The author makes no statement as to whether the amygdales formed from residual magmatic fluids or from metasomatic fluids percolating through the rocks at some later date. The only conclusion is that their formation is not penecontemporaneous with the final crystallization of the flow.

Application to the Metamorphic Facies Concept

The concept of metmorphic facies was first formally proposed in 1893 when Barrow described an intrusion of biotite-muscovite gneiss in the southeast highlands of Scotland and its accompanying metamorphism. Since that time considerable work has been done on the classification of metamorphic facies. Figure 25 illustrates the present state of knowledge with respect to the classification of metamorphic facies and shows that the classification is still in a state of flux. The recent development of prehnite as an index mineral for low-grade or burial metamorphism is particularly noteworthy here.

Fyfe et al. (1958) first defined the zeolite facies as transitional rocks between diagenesis and metamorphism. This original definition was based on Coomb's (1954) description of altered andesitic volcanic sands buried to depths of 6-9 km in Southland, New Zealand. This depth would correspond to a load pressure of 2000-3000 atmospheres and a temperature of 200-300°C. Since its introduction in 1958,

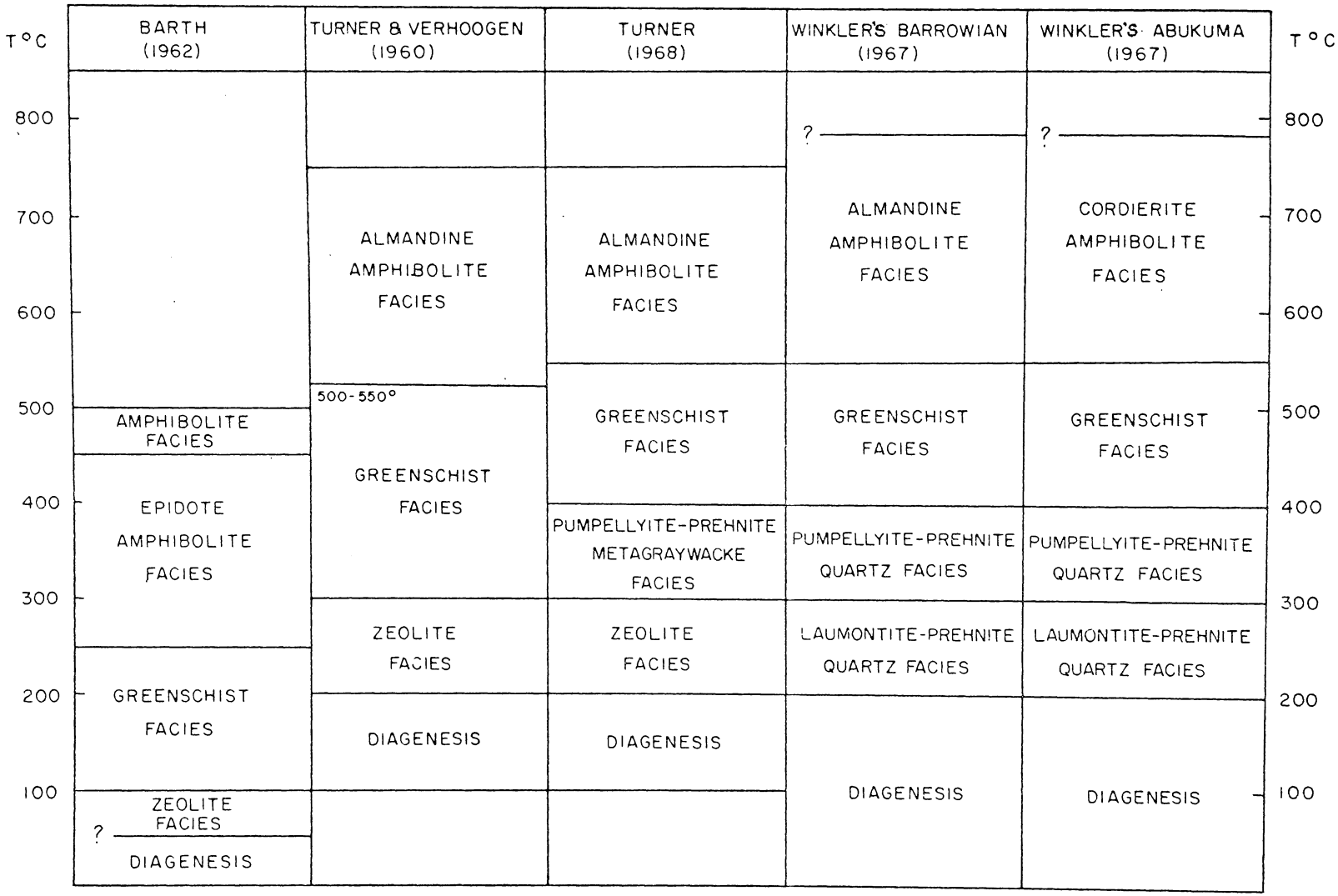

Figure 25. Compilation of Low-grade Region Metamorphism Classifications

the zeolite facies has undergone a metamorphism of its own. This is based primarily on the fact that it has recently been recognized throughout the world in rocks that have undergone low-grade or burial metamorphism. This evolution of the zeolite facies has brought interest to the zeolite group of minerals and other minerals, such as prehnite, which are associated with them.

Turner (1968) and Winkler (1967) have defined metamorphic facies which are named for the occurrence of prehnite, as well as pumpellyite and laumontite. Both investigators use these phases as the index minerals which define the facies in which they occur. The pumpellyite-prehnite-quartz facies of Winkler (1967) differs from the pumpellyite-prehnite-metagraywacke facies of Turner (1968) in name only. Winkler holds that because the mineral assemblage producing these facies is present in rocks other than metagraywackes, it would be misleading to use the term metagraywacke in the name of the facies. Because the two classifications are the same, except in the use of terminology, Winkler's more specific terminology will be used.

The lower limit of the laumontite-prehnite-quartz facies is marked by the reaction of heulandite to form laumontite and the reaction of anacline + quartz to form albite. The equilibrium conditions of the pertinent reactions are not sufficiently well established to accurately determine the temperature and pressure conditions for the beginning of metamorphism, although Winkler (1967) states that the temperatures on the order of 200^{o}C must be attained for the onset of the laumontite-prehnite-quartz facies. The upper limit of the laumontite-prehnite-quartz facies is reached when laumontite disappears. The dissociation

temperature of isolated laumontite has been determined to be 410°C at 1000 bars water pressure (Koisumi and Roy, 1960). Winkler (1967) points out that laumontite should dissociate at a much lower temperature when in the presence of other phases with which it can react. Therefore, he arbitrarily sets the upper limit of the laumontite-prehnite-quartz facies at 300°C (Fig. 25). This disappearance of laumontite at the upper limit of the laumontite-prehnite-quartz facies also marks the lower limit of the pumpellyite-prehnite-quartz facies. The upper limit of the pumpyllyite-prehnite-quartz facies or the lower limit of the greenschist facies is marked by the disappearance of prehnite and pumpellyite and the appearance of zoisite, epidote, and actinolite. Although the assignment of a temperature for this transition is purely arbitrary, Winkler sets the upper limit on the pumpellyite-prehnite-quartz facies at 400°C.

The prehnite dissociation curve (Fig. 11) shows that prehnite decomposes at 475°C at 1000 bars water pressure. This is 75°C higher than the upper limit of the pumpellyite-prehnite-quartz facies as established by Winkler. It is concluded that prehnite should and does dissociate at a much lower temperature when in the presence of other phases with which it can react, as shown by the formation of grossularite. Samples prepared with equal mole percents of prehnite and calcite caused a decomposition of the prehnite at temperatures as much as 100°C below the decomposition curve of isolated prehnite.

Isolated metamorphism of prehnite or laumontite is probably not realistic in nature. The prehnite plus vapor field would be within the laumontite-prehnite-quartz facies or the pumpellyite-prehnite-quartz facies, whereas the anorthite plus wollastonite plus vapor field would

fall in the sanidinite facies. The sanidinite facies is the only metamorphic facies in which anorthite and wollastonite can coexist (Winkler, 1967). To go from the pumpellyite-prehnite-quartz facies directly to the sanidinite facies seems unrealistic, and without any other phases being present in nature, this is what we would see. Therefore, it is concluded that natural prehnite does not decompose directly to wollastonite and anorthite but reacts with other phases and forms other products.

Further experimentation in this area is essential to fully understand the parameters controlling the decomposition or disappearance of these minerals in metamorphic rocks. It is necessary to experimentally determine the stability of mineral assemblages in order to expand our knowledge of the metamorphic facies. Some simple but meaningful assemblages that need to be studied are the following:

Prehnite + Calcite $\rightleftharpoons$ Grossularite

Prehnite + Calcite + Quartz $\rightleftharpoons$?

Prehnite + Quartz $\rightleftharpoons$?

Laumontite + Calcite $\rightleftharpoons$ Prehnite + Quartz

Laumontite + Quartz + Calcite $\rightleftharpoons$?.

It is concluded that prehnite is a poor index mineral in light of the known data. This investigation has shown that its stability is greatly dependent upon composition and therefore cannot be relied upon to clearly define pressure-temperature conditions in the compositionally variant systems of natural rocks. Further studies may show that a prehnite-quartz or prehnite-calcite assemblage may be compositionally less dependent upon pressure. Figure 11 shows that prehnite may decompose at

temperatures from 100°C to over 500°C depending upon the pressure. Until further experimental work is completed using mineral assemblages, the use of prehnite as an index mineral does not seem to be substantiated.

REFERENCES

Baker, G., 1953, Ilaite and prehnite in micropegmatitic diorite, southeast Papua: Am. Mineralogist, v. 38, p. 840-944.

Barth, T. F. W., 1962, Theoretical petrology: New York, John Wiley & Sons, 416 p.

Burnham, C. W., 1959, Contact metamorphism of magnesian limestones at Crestmore, California: Geol. Soc. America Bull., v. 70, p. 879-919.

Coombs, D. W., 1954, The nature and alteration of some Triassic sediments from Southland, New Zealand; Roy. Soc. New Zealand Trans., v. 82, p. 65-109.

_____1960, Lower grade mineral facies in New Zealand: Geol. Cong., 21st, Copenhagen, 1960, Sec., v. 13, p. 339-351.

_____, Ellis, A. J., Fyfe, W. S., and Taylor, A. M., 1959, The zeolite facies; with comments on the interpretation of hydrothermal synthesis: Geochim. et Cosmochim. Acta, v. 17, p. 53-107.

Deer, W. A., Howie, R. A., and Zussman, J., 1962, Rock forming minerals, Vol. 3, Sheet silicates: New York, John Wiley & Sons, 270 p.

Eskola, P., 1934, Prehnite amygdaloid from the bottom of the Baltic: Mineralogical Mag., abs., v. 24, p. 25.

Fraser, D. M., Butler, R. D., and Hurlbut, C. S., 1938, Prehnite from Coopersburg, Pennsylvania: Am. Mineralogist, v. 23, p. 583-587.

Fyfe, W. S., Turner, F. J., and Verhoogen, J., 1958, Metamorphic reactions and metamorphic facies: Geol. Soc. America, Mem. 73, 259 p.

Gallitelli, P., 1928, Sulla prehnite di Toggiano: Soc. Toscana Sci. Nat. Atti, v. 38, p. 267-273.

Goldsmith, J. R., 1952, Synthesis of soda-free thomsonite: Mineralogical Mag., v. 29, p. 952-954.

Gossner, B., and Mussgnug, F., 1931, Rontgenographische Untersuchsung und Prehnit und Lawsonite: Centr. Min. Abt. A., p. 419-423.

Greenwood, J. J., 1962, Carnegie Inst. Washington Yearbook 61, p. 82-85.

Hall, A., 1964, The occurrence of prehnite in apinitic rocks from Donegal, Ireland: Mineralogical Mag., v. 35, p. 234-236.

Handbook of Physics and Chemistry (R. C. Weast, ed.), 1968, Cleveland, The Chemical Rubber Company.

Harker, R. I., and Tuttle, O. F., 1956, Experimental data on the P_{CO_2}-T curve for the reaction: calcite + quartz wollastonite + carbon dioxide: Am. Jour. Sci., v. 254, p. 239-256.

Kennedy, G. C., 1950a, Pressure-volume-temperature relations in water at elevated temperatures and pressures: Am. Jour. Sci., v. 248, p. 540-564.

_____1950b, A portion of the system silica-water: Econ. Geology, v. 45, p. 629-653.

_____, and Holser, W. T., 1966, P-V-T and phase relations of water and carbon dioxide: Geol. Soc. America, Mem. 97, p. 371-383.

Kerr, P. F., 1959, Optical mineralogy: New York, McGraw-Hill Book Company, Inc., 442 p.

Koisumi, M., and Roy, R., 1960, Zeolite studies. I. Synthesis and stability of the calcium zeolites: Jour. Geology, v. 68, p. 41-53.

Kupletsky, B. M., 1925, Sur une roche a prehnite des Monts Botogol en Siberie: Mineralogical Mag., abs., v. 21, p. 85-87.

Lowenstein, W., 1954, The distribution of aluminum in the tetrahedra of silicates and aluminates: Am. Mineralogist, v. 39, p. 92-96.

Luth, W. C., and Ingamells, C. O., 1965, Gel preparation of starting materials for hydrothermal experimentation: Am. Mineralogist, v. 50, p. 255-258.

Nuffield, E. W., 1943, Prehnite from Ashcroft, British Columbia; Univ. Toronto Stud., Geol. Ser., no. 48, p. 49-64.

Papike, J. J., and Zoltai, T., 1967, Ordering of tetrahedral aluminum in prehnite: Am. Mineralogist, v. 52, p. 974-984.

Peng, S., Chou, K., and Tang, Y., 1959, Structure of prehnite: Acta Chim. Sinica, v. 25, p. 56-63.

Preisinger, A., 1965, Prehnite--ein neuer Schichtsilikattyp: Tschm. Mineral Petrogr. Mitt., v. 10, no. 1-4, p. 491-504.

Richmond, W. E., 1938, Paragenesis of the minerals from Blueberry Mountain, Woburn, Massachusetts: Am. Mineralogist, v. 22, p. 407-423.

Seki, Y., 1961, Pumpellyite in low-grade metamorphism: Jour. Petrology, v. 2, p. 407-423.

Simpson, D. R., 1969, Prehnite veins in Triassic diabase, Coopersburg, Pennsylvania: Geol. Soc. America Bull., v. 80, p. 1355-1361.

Smith, J. V., and Bailey, S. W., 1963, Second review of Al-O Si-O tetrahedral distances: Acta Crystallogr., v. 16, p. 801-811.

Surdam, R. C., 1969, Electron microprobe study of prehnite and pumpellyite from the Karmutsen Group, Vancouver Island, British Columbia: Am. Mineralogist, v. 54, p. 256-266.

Taylor, J. H., 1935, A contact metamorphic zone from the Little Belt Mountains, Montana: Am. Mineralogist, v. 20, p. 120-128.

Traube, H., 1894, Uber die pyroelektrischen Eigenschaften und die Krystallformen des Prehnits: Neues Jahrb. Mineral, v. 9, p. 134-146.

Turner, F. J., 1968, Metamorphic petrology--Mineralogy and field aspects: New York, McGraw-Hill Book Company, Inc., 403 p.

_____, and Verhoogen, J., 1960, Igneous and metamorphic petrology: New York, McGraw-Hill Book Company, Inc., 694 p.

Tuttle, O. F., 1949, Two pressure vessels for silicate-water studies: Geol. Soc. America Bull., v. 60, p. 1727-1729.

Watson, K. D., 1953, Prehnitization of albitite: Am. Mineralogist, v. 38, p. 197-206.

Watters, W. A., 1964, Prehnitization in the Yagan Formation of Navarino Island, southermost Chile: Mineralogical Mag., v. 34, p. 517-527.

Winkler, H. G. F., 1967, Petrogenesis of metamorphic rocks: New York, Springer-Verlag New York Inc., 237 p.